Generalization of Applications of Free Molecule Flow

by I. M. Garfunkel

Project MX-794
USAF Contract W33-038-ac-14222

Willow Run Research Center
Engineering Research Institute
University of Michigan
UMM-55 July 1950

TABLE OF CONTENTS

ABSTRACT

The derivation of the free molecule expressions for shear and normal pressure on an element of surface inclined at angle θ with the free stream is shown. These expressions are then used to develop a general procedure for finding lift and drag on any of a restricted class of bodies at all angles of attack. This general theory is then applied to four specific bodies of revolution: semi-infinite right circular cone, infinite right circular cylinder, prolate ellipsoid, and double ogive. A fifth application is made in obtaining drag and lift curves for a body composed of an ogive plus half a prolate ellipsoid at angles of attack of 0° and 45°.

LIST OF SYMBOLS

α	- Angle of attack
A	- Planform area at zero angle of attack
β	- Angle between the free stream vector and the normal to a general surface element
$c_i = \sqrt{2RT_i}$	- Most probable velocity of the molecules in the impinging stream
$c_r = \sqrt{2RT_r}$	- Most probable velocity of the molecules in thermal equilibrium at a temperature T_r of the re-emitted gas
$C_D = \frac{D}{qA}$	- Coefficient of drag
$C_L = \frac{L}{qA}$	- Coefficient of lift
D	- Drag
dS	- General element of surface area
$\mathrm{erf}(t) = \frac{2}{\sqrt{\pi}} \int_0^t e^{-s^2} ds$	- Error function of t
F	- Total force on a body
F_x, F_y, F_z	- x, y, z components of force on a body
$\gamma = \frac{c_p}{c_v}$	- Ratio of specific heats
G (x,y,z)	- Mathematical expression for the shape of an arbitrary body

LIST OF SYMBOLS (CONTINUED)

G_x, G_y, G_z	- Direction numbers of the normal to a general surface element
Γ	- $-\sqrt{G_x^2 + G_y^2 + G_z^2}$
$\Gamma_x = \frac{G_x}{\Gamma}$	- Cosine of the angle between the normal to a surface element and the x-axis
L	- Lift
λ, μ, ν	- Direction cosines of the free stream velocity vector U
$M_\infty = \frac{U}{c_i}$	- Molecular speed ratio
$p(\theta)$	- Normal pressure on an element of surface inclined at angle θ with the free stream.
$q = \frac{1}{2}\rho U^2$	- Dynamic pressure
R_1	- Universal gas constant, related to "ordinary" gas constant R by: $R_1 = \frac{R}{W}$
T_i	- Temperature of the impinging stream
T_r	- Temperature of the re-emitted stream
T_x, T_y, T_z	- Direction cosines of the tangent to a general element of surface (in the plane of the velocity vector U and the normal Γ)
$\tau(\theta)$	- Shear stress on an element of surface inclined at angle θ with the free stream
θ	- Angle between a surface element and the free stream velocity

LIST OF SYMBOLS (CONTINUED)

U	- Free stream velocity
W	- Molecular weight
x, y, z	- Space variables

I. INTRODUCTION

Free molecule flow is defined as the flow (past a solid surface) of a fluid of very low density, such that the mean free path of the free stream molecules is large compared with the linear dimensions of the surface being considered. As a consequence, the collisions of the molecules of the free stream with each other have no effect whatever on the free stream velocity, and the force opposing the motion of the fluid past the surface is due solely to the action of the molecules of the fluid upon the surface. If we now also assume that the medium in which a body is being considered is composed of small spherical molecules, the concepts of kinetic theory apply.

In free molecule flow, the action of the molecules may be considered to be characterized by three different reflection phenomena:

A. Specular Reflection - in which the component of molecular velocity tangent to the element of surface from which the molecule is reflected remains unchanged, while the normal component reverses its direction; there is no adjustment of gas temperature to that of the surface of the body.

B. Diffuse Reflection - in which the molecules of the gas are momentarily adsorbed, (thus, one of the boundary conditions is in terms of a derivative with respect to time), so that the direction of the motion of the reflected molecules is completely unrelated to the direction of the impinging stream. This type of reflection is accompanied by an exchange of evergy between the molecules of the stream and the body surface expressible in terms of an accomodation coefficient Θ, a measure of the extent to which reflected or re-emitted molecules have their energy adjusted toward that of an equivalent mass of gas traveling in a stream at the temperature of the surface. This "accommodation" of the temperature of the impinging stream toward that of the wall is due to the momentary adsorption of the gas molecules by the surface, hence is dependent on the average length of time elapsing before re-emission. Weidman determined the value of Θ for air on metals, and concluded that its value is independent of the nature of the metal surface (Ref. 9).

Along with the energy exchange, diffuse reflection is accompanied by a momentum exchange expressible in terms of f, Maxwell's coefficient, which is the fraction of tangential momentum of the oncoming molecules transferred to the wall upon collision. A table showing that values of f are usually very nearly unity for all materials at present deemed suitable for rocket "skins" is given by Millikan (Ref. 10). Therefore, it might be expected that diffuse reflection may account for practically all the action of the molecules on the body.

C. Uniform Adsorbed Layer - an "in between" case in which the impinging molecules form an adsorbed layer, and later "evaporate" in such a manner that no contribution to resultant forces or moments arises when the molecules are re-emitted. There is a pressure due to the re-emission from the layer, but it is distributed so that the contribution of any one part of a body is just cancelled by the contribution of the rest of the body, so that all the forces we need deal with are those needed to bring the molecules to rest with respect to the missile surface. Thus, temperature adjustment is not a factor to be considered in the calculation of these forces.

Although it might prove difficult to realize this mechanism physically, use of the concept can lead to simplification of results without greatly impairing the accuracy of the calculations involved.

The "cosine law" of reflection, that the number of molecules leaving a surface element in any direction is proportional to the cosine of the angle between the direction and the normal to the surface element, expresses the result of numerous molecular ray experiments. As long as the de Broglie wave length of the incident molecules is large compared with the average roughness height times the sine of the angle of incidence, specular reflection is not observed, nor expected by theory; thus the possibility of occurrence of specular reflection is limited to angles of incidence very near grazing. Although the tendency to grazing angles of incidence increases at high Mach number, it can be shown that, at high Mach number, the increase in tendency to grazing incidence is almost exactly offset by the decrease in de Broglie wave length. For all ranges of Mach number, ignoring the effect of specular reflection will introduce an error of less than half a percent into the calculation of restoring force (Ref. 3).

II. PRESSURE ON AN ELEMENT OF SURFACE

As mentioned above, the collisions of the fluid particles with each other have no effect whatever on the free stream velocity; so the total effect of a stream of molecules might be found by adding the effect of collision by each molecule separately for all the molecules. In subsequent discussion, all quantities are assumed to be averages.

The following closely parallels the development presented by Tsien (Ref. 4) and Ashley (Ref. 5).

Letting u', v', and w' be the velocity components of a molecule in directions x', y', and z' fixed relative to U (the free stream motion of the fluid), and if collisions between molecules and other mutual forces are neglected, then the kinetic theory states that the molecular velocity distribution is Maxwellian, i.e., the number of molecules per unit volume with velocities in the range u' to (u' + du'), v' to (v' + dv'), w' to (w' + dw'), is

$$N_{u,v,w}\,du'\,dv'\,dw' = dN' = N\left(\frac{h}{\pi}\right)^{\frac{3}{2}} e^{-h(u'^2+v'^2+w'^2)}\,du'\,dv'\,dw' \qquad (1)$$

where

N = number of molecules per unit volume.

$$N_{uvw} = N\left(\frac{h}{\pi}\right)^{\frac{3}{2}} e^{-h(u'^2+v'^2+w'^2)}$$

$$h = \frac{1}{2RT_i} = \frac{1}{c_i^2}$$

c_i = most probable velocity of the molecules in the free stream

If unit area dS of a plane surface S moves with velocity components $\lambda' U$, $\mu' U$, $\nu' U$ in directions x', y', z', then, in the relative coordinate system fixed in the plane surface such that x is the outward normal to the surface, the velocities u, v, w in directions x, y, z are

$u = u' - \lambda' U$)
$v = v' - \mu' U$)   where λ', μ', ν' are the direction cosines of U in the x' y' z' system.
$w = w' - \nu' U$)

Then the number of molecules with velocity components in the range u to u + du, v to v + dv, w to w + dw, is

$$N_{u,v,w}\, du\, dv\, dw = dN = N\left(\frac{h}{\pi}\right)^{\frac{3}{2}} e^{-h\left[(u+\lambda' U)^2 + (v+\mu' U)^2 + (w+\nu' U)^2\right]} du\, dv\, dw \qquad (2)$$

In unit time, the molecules (with velocity components in the specified range) that strike the surface dS, are contained in a cylinder with dS as base, slant height $\sqrt{u^2 + v^2 + w^2}$, and altitude -u (-u because only molecules with x velocities in the negative range $-\infty < u < 0$ can strike the surface dS). Since the volume of the cylinder is -udS, the number of these molecules striking unit area of S is then $-uN_{uvw}dudvdw = -udN$. The total number n of molecules striking this unit area is then the integrated sum of -udN over all possible velocities of impinging molecules.

$$n = -N\left(\frac{h}{\pi}\right)^{\frac{3}{2}} \int_{-\infty}^{0} du \int_{-\infty}^{\infty} dv \int_{-\infty}^{\infty} u e^{-h\left[(u+\lambda' u)^2 + (v+\mu' v)^2 + (w+\nu' u)^2\right]} dw$$

$$= \frac{N}{2}\left\{\frac{e^{-h\lambda'^2 U^2}}{\sqrt{\pi h}} + \lambda' U\left[1 + \operatorname{erf}(\lambda' U\sqrt{h})\right]\right\} \qquad (3)$$

where erf (t) represents the conventional error function of statistical theory, defined by

$$\operatorname{erf}(t) = \frac{2}{\sqrt{\pi}} \int_0^t e^{-\beta^2} d\beta$$

Multiplying equation (3) by the average mass, m, per molecule ($mN = \rho$, free stream density), the mass m_i of the stream striking unit area per second of the plate is:

$$m_i = \frac{\rho}{2}\left\{\frac{e^{-h\lambda'^2 U^2}}{\sqrt{\pi h}} + \lambda' U\left[1+\mathrm{erf}(\lambda' U\sqrt{h})\right]\right\} \tag{4}$$

The total momentum of the stream of mass m_i in an arbitrary direction specified by direction cosines λ_1, μ_1, ν_1, is found by integrating the momenta of molecules in each velocity range:

$$M_{\lambda_1,\mu_1,\nu_1} = -\rho\left(\frac{h}{\pi}\right)^{\frac{3}{2}}\int_{-\infty}^{0}du\int_{-\infty}^{\infty}dv\int_{-\infty}^{\infty}u(\lambda_1 u+\mu_1 v+\nu_1 w)\,e^{-h\left[(u+\lambda' U)^2+(v+\mu' U)^2+(w+\nu' w)^2\right]}dw$$

$$= \frac{-\rho U^2}{2}\left\{\frac{(\lambda'\lambda_1+\mu'\mu_1+\nu'\nu_1)\,e^{-\lambda'^2U^2h}}{U\sqrt{\pi h}} + \left[\frac{\lambda_1}{2hU^2}+\lambda'(\lambda'\lambda_1+\mu'\mu_1+\nu'\nu_1)\right]\left[1+\mathrm{erf}(\lambda' U\sqrt{h})\right]\right\} \tag{5}$$

For calculating the pressure p_i due to impact of molecules on a plane inclined at angle θ to the free stream velocity U,

$$\lambda' = \mathrm{Sin}\,\theta \qquad \lambda_1 = -1$$
$$\mu' = \mathrm{Cos}\,\theta \qquad \mu_1 = 0$$
$$\nu' = 0 \qquad \nu_1 = 0$$

Substituting these into equation (5):

$$\frac{p_i(\theta)}{\frac{1}{2}\rho U^2} = \frac{\mathrm{Sin}\,\theta}{\sqrt{\pi}}\,\frac{c_i}{U}\,e^{-\frac{U^2}{c_i^2}\mathrm{Sin}^2\theta} + \left(\frac{c_i^2}{2U^2}+\mathrm{Sin}^2\theta\right)\left[1+\mathrm{erf}\left(\frac{U}{c_i}\mathrm{Sin}\,\theta\right)\right] \tag{6}$$

When U = 0 (for a gas at rest), $p_i = \frac{1}{4}\rho c_i^2$, which is half that yielded by the kinetic theory, the other half being due to reflection. For $U \gg c_i$ and $\theta = 90^\circ$, $p_i = \frac{1}{2}\rho c_i^2 + \rho U^2$, which checks with the result of Zahm (Ref. 1), except for a factor of 2, since we have found only pressure due to impact and not the total pressure.

Substituting $M_\infty = U\sqrt{h} = \frac{U}{\sqrt{2RT_i}} = \frac{U}{c_i}$, equation (6) becomes:

$$\frac{p_i(\theta)}{\frac{1}{2}\rho U^2} = \frac{\sin\theta}{M_\infty\sqrt{\pi}}\, e^{-M_\infty^2 \sin^2\theta} + \left(\frac{1}{2M_\infty^2} + \sin^2\theta\right)\left[1 + \operatorname{erf}(M_\infty \sin\theta)\right] \qquad (6a)$$

If the stream of molecules is first absorbed by the surface before reflection, all the tangential momentum is transferred to the surface; to calculate the shearing stress τ_i thus produced, the direction cosines are:

$$\lambda' = \sin\theta \qquad \lambda_1 = 0$$
$$\mu' = \cos\theta \qquad \mu_1 = -1$$
$$\nu' = 0 \qquad \nu_1 = 0$$

Substituting into equation (5):

$$\frac{\tau_i(\theta)}{\frac{1}{2}\rho U^2} = \frac{\cos\theta}{M_\infty\sqrt{\pi}}\, e^{-M_\infty^2 \sin^2\theta} + \sin\theta\cos\theta\left[1 + \operatorname{erf}(M_\infty \sin\theta)\right] \qquad (7)$$

If the reflection of molecules is specular, the component of motion of the incoming molecules normal to the reflecting surface is simply reversed in direction, while the tangential component remains unchanged. Then the pressure due to re-emission is $p_r = p_i$, and the shearing stress due to re-emission is $\tau_r = -\tau_i$. If, however, reflection is diffuse, no preferred direction of re-emission exists, so $\tau_r = 0$, and total tangential stress. $\tau = \tau_i + \tau_r = \tau_i$.

To determine the pressure p_r due to diffuse re-emission, we must use the fact (as shown in texts (Ref. 11) on kinetic theory) that

$$p_r = \frac{\sqrt{\pi}}{2} c_r m_r$$

where

$c_r = \sqrt{2RT_r}$ = most probable velocity of the re-emitted molecules

m_r = mass emitted per second per unit area.

For steady state reflection, m_r must equal m_i given by equation (4).

Then

$$\frac{p_r(\theta)}{\frac{1}{2}\rho U^2} = \frac{1}{2M_\infty^2}\,\frac{C_r}{C_i}\,e^{-M_\infty^2 \sin^2\theta} + \frac{\sqrt{\pi}}{2}\,\frac{\sin\theta}{M_\infty}\,\frac{C_r}{C_i}\left[1+\mathrm{erf}(M_\infty \sin\theta)\right]$$

$$= \sqrt{\frac{T_r}{T_i}}\left\{\frac{e^{-M_\infty^2 \sin^2\theta}}{2M_\infty^2} + \frac{\sqrt{\pi}}{2}\,\frac{\sin\theta}{M_\infty}\left[1+\mathrm{erf}(M_\infty \sin\theta)\right]\right\} \tag{8}$$

since

$$\frac{C_r}{C_i} = \frac{\sqrt{2RT_r}}{\sqrt{2RT_i}} = \sqrt{\frac{T_r}{T_i}}$$

The total pressure due to both impinging and re-emission, with f fraction of the molecules reflected diffusely and (1-f) specularly, is:

$$\frac{p}{\frac{1}{2}\rho U^2} = (2-f)\frac{p_i}{\frac{1}{2}\rho U^2} + f\,\frac{p_r}{\frac{1}{2}\rho U^2} \tag{9}$$

Similarly, the shearing stress is:

$$\frac{\tau}{\frac{1}{2}\rho U^2} = f\,\frac{\tau_i}{\frac{1}{2}\rho U^2} \tag{10}$$

If f is assumed to be 1 (reflection is all diffuse),

$$\frac{p}{\frac{1}{2}\rho U^2} = \frac{p_i}{\frac{1}{2}\rho U^2} + \frac{p_r}{\frac{1}{2}\rho U^2} \tag{9a}$$

So far as is known at present, f is independent of angle of attack θ, so it does not complicate any integrations of p or τ over θ.

A table may now be drawn up, showing the pressures and stresses that must be accounted for for each reflection mechanism mentioned above:

Table of Pressures on an Element of Unit Area

Reflection / Pressure	Specular	Uniform Adsorbed Layer	Diffuse
Normal	$\frac{p}{q} = \frac{2p_i}{q}$	$\frac{p}{q} = \frac{p_i}{q}$	$\frac{p}{q} = \frac{p_i}{q} + \frac{p_r}{q}$
Shear	$\frac{\tau}{q} = 0$	$\frac{\tau}{q} = \frac{\tau_i}{q}$	$\frac{\tau}{q} = \frac{\tau_i}{q}$

Since, as pointed out earlier, specular reflection has a negligible influence upon calculation of drag and lift, we shall henceforward direct our attention to the other two mechanisms.

Experimental data indicate that according to certain specific criteria, a body in flight may (depending on its velocity) pass into the free molecule flow regime at altitudes as low as five hundred thousand feet. (Ref. 2, 7 and 8). For bodies at those altitudes and above, such evidence as exists leads to the belief that the energy of the molecules of the incident stream generally exceeds that of the re-emitted stream. If we take unity as the value of the upper limit of the ratio $\frac{c_r}{c_i}$, then presumably the maximum value of restoring force is calculated by the mechanism of diffuse reflection: this we call "extreme" diffuse reflection.

Conveniently enough, determination of force in the case of uniform adsorbed layer is identically that for diffuse reflection, when the ratio $\frac{c_r}{c_i}$, is arbitrarily assigned the value zero. This presumably is the minimum value that restoring force may be. (N.B.: The physical quantities represented by c_r and T_r can never be identically zero in any physical case; they are merely arbitrarily assigned that value in the case of uniform adsorbed layer to aid in simplifying the mathematical formulation of the maximum range of restoring force encountered in free molecule flow, i.e., as a simple means of bracketing the total range expected by theory.)

Then the pressures (shear and normal) arising in diffuse reflection can be made to bracket the whole range of pressures expected by theory by letting the ratio $\frac{c_r}{c_i}$ take on all values from 0 to 1. However, when we say $\frac{c_r}{c_i} = 0$, we really mean $p_r = 0$ as used above in describing the mechanism of uniform adsorbed layer.

III. BODIES AT ARBITRARY ANGLE OF ATTACK

A. INTRODUCTION

In general, except for simple configurations at zero angle of attack, force components on a body can be evaluated only by numerical integration. Exposition and illustration of one of the methods involved in integrating numerically may be found in Section IV of this paper.

Three of the bodies considered here have been dealt with in the case of zero angle of attack by Ashley (Ref. 5 and 6). When the treatment given here is specialized to $\alpha = 0$, the results reduce identically to those obtained by Ashley.

The following analysis is exactly valid only when the flow is uniform, assumed of infinite extent, and if the body under consideration is such that a tangent to the surface at any point does not intersect the body surface.

B. GENERAL METHOD

Given a body subject to the above conditions, orient it such that a convenient point is the origin, and the space coordinate axes coincide with axes of symmetry (if such exist) of the body. Express the shape of the body mathematically in terms of a function G(x,y,z) of the space variables, and find the partial derivatives G_x, G_y, G_z which are the direction numbers of the normal to a general surface element of the body. The direction cosines of the normal are $\Gamma x, \Gamma y, \Gamma z$, where

$$\Gamma_x = \frac{G_x}{\Gamma}$$

$$\Gamma_y = \frac{G_y}{\Gamma}$$

$$\Gamma_z = \frac{G_z}{\Gamma}$$

$$\Gamma = \sqrt{G_x^2 + G_y^2 + G_z^2} \qquad (1)$$

If the flow is such that the free stream has direction cosines (λ, μ, ν), the angle β between the free stream vector and the normal is given by:

$$\cos\beta = \lambda\Gamma_x + \mu\Gamma_y + \nu\Gamma_z \qquad (2)$$

and the surface element may be considered to be at angle of attack $(\frac{\pi}{2} - \beta)$ with the free stream, so that $\frac{p\left(\frac{\pi}{2} - \beta\right)}{q}$ and $\frac{\tau\left(\frac{\pi}{2} - \beta\right)}{q}$ are the free molecule normal and shear pressures, respectively, on the surface element in question.

Then the force components are to be found by integrating these pressures over the surface of the body in free molecule flight as follows:

$$F_x \text{ (X componet of force)} = q\int_s \left[\frac{p(\frac{\pi}{2}-\beta)}{q}\Gamma_x + \frac{\tau(\frac{\pi}{2}-\beta)}{q}T_x\right] ds$$

$$F_y = q\int_s \left[\frac{p(\frac{\pi}{2}-\beta)}{q}\Gamma_y + \frac{\tau(\frac{\pi}{2}-\beta)}{q}T_y\right] ds$$

$$F_z = q\int_s \left[\frac{p(\frac{\pi}{2}-\beta)}{q}\Gamma_z + \frac{\tau(\frac{\pi}{2}-\beta)}{q}T_z\right] ds \qquad (3)$$

where T_x, T_y, T_z are the direction cosines of that tangent to a general element of surface which is in the plane of the velocity vector U and the normal Γ, and are themselves determined by means of the following equations:

$$\Gamma_x T_x + \Gamma_y T_y + \Gamma_z T_z = 0$$
$$\lambda T_x + \mu T_y + \nu T_z = \sin\beta$$
$$T_x^2 + T_y^2 + T_z^2 = 1$$

(4)

The total restoring force on the body may then be found by summing vectorially:

$$F = \sqrt{F_x^2 + F_y^2 + F_z^2} \qquad (5)$$

along a line with direction cosines $\frac{F_x}{F}, \frac{F_y}{F}, \frac{F_z}{F}$,

Then the lift L and drag D act in the plane determined by the vectors F and U.

$$D = F \cos (\vec{F}, \vec{U})$$

$$L = F \sin (\vec{F}, \vec{U}) \tag{6}$$

$$C_D = \frac{D}{qA}$$

$$C_L = \frac{L}{qA} \tag{7}$$

where A is the planform area at zero angle of attack, although the reference area may be chosen arbitrarily, so long as it is treated consistently.

C. GENERAL BODIES OF REVOLUTION

If the body we are dealing with is a body of revolution, the axis of revolution is an axis of symmetry. If we orient the body so that its axis of symmetry lies along the x-axis, we may, without loss of generality, restrict the free stream vector to, say, the x- y- plane. Its direction cosines then are cos α, sin α, 0 where α is the angle between the free stream velocity U and the x-axis. Then the pressure components in the z-direction when summed over the surface of the body just cancel each other, so that the resultant force F acts in the plane determined by U and the x-axis; i.e., as mentioned above, in the x- y- plane. Then (3) becomes:

$$\frac{F_z}{q} = \int_S \left[\frac{p\left(\frac{\pi}{2} - \beta\right)}{q} \Gamma_z + \frac{\tau\left(\frac{\pi}{2} - \beta\right)}{q} T_z \right] ds = 0 \tag{3a}$$

by symmetry, because of the choice of coordinate axes.

Then (6) becomes:

$$D = F \cos(\phi - \alpha)$$

$$L = F \sin(\phi - \alpha) \qquad (6a)$$

where ϕ is the angle between F and the x-axis.

D. APPLICATION TO SPECIFIC BODIES OF REVOLUTION

1. Infinite right circular cylinder of radius R at angle of attack α:*

$$G(x, y, z) = x^2 + z^2 - R^2 = 0$$

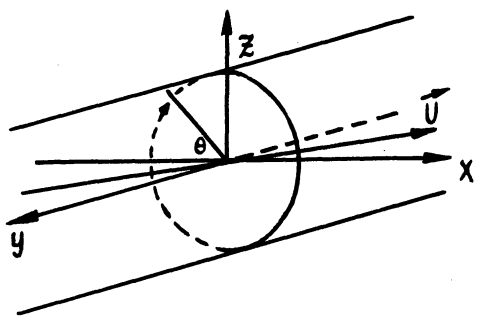

Parametric representation:

$$x = -R\cos\theta$$
$$z = R\sin\theta$$
$$y = y \qquad (1)$$

$$G_x = 2x, \quad G_y = 0, \quad G_z = 2z, \quad \Gamma = -2R,$$

$$\Gamma_x = \cos\theta, \quad \Gamma_y = 0, \quad \Gamma_z = -\sin\theta, \qquad (2)$$

U is parallel to x- y- plane; direction cosines are: $\cos\alpha$, $\sin\alpha$, 0.

*For convenience, we set up the coordinate system as follows: at zero angle of attack, the free stream vector is normal to the axis of the cylinder. Therefore, the x- y- plane is rotated through 90°, so that the axis of symmetry of the body lies on the y-axis, instead of along x, as in III C.

Then: $\cos\beta = \cos\alpha \cos\theta$ (3)

$$\frac{ds}{A} = \frac{\ell R d\theta}{2R\ell} = \tfrac{1}{2} d\theta \qquad (4)$$

$$\left.\begin{aligned} T_x &= \frac{\cos\alpha \sin^2\theta}{\sin\beta} \\ T_z &= \frac{\cos\alpha \sin\theta \cos\theta}{\sin\beta} \\ T_y &= \frac{\sin\alpha}{\sin\beta} \end{aligned}\right\} \qquad (5)$$

Then:

$$F_x = qA\int_0^{\pi}\left[\frac{p(\frac{\pi}{2}-\beta)}{q}\cos\theta + \frac{\tau(\frac{\pi}{2}-\beta)}{q}\,\frac{\cos\alpha \sin^2\theta}{\sin\beta}\right]d\theta \qquad (6)$$

$$F_y = qA\sin\alpha\int_0^{\pi}\frac{\tau(\frac{\pi}{2}-\beta)}{q}\,\frac{d\theta}{\sin\beta} \qquad (7)$$

$F = \sqrt{F_x^2 + F_y^2}$ at $\varphi = \arctan \dfrac{F_y}{F_x}$ in the x- y- plane

$$\left.\begin{aligned} C_D &= \frac{D}{qA} = \frac{F}{qA}\cos(\phi - \alpha) \\ C_L &= \frac{L}{qA} = \frac{F}{qA}\sin(\phi - \alpha) \end{aligned}\right. \qquad (8)$$

At $\alpha = 0$,

then: $\cos\beta = \cos\theta,\ d\beta = d\theta,\ \beta = \theta$ (9)

$$T_x = \sin\beta,\ T_z = \cos\theta,\ T_y = 0 \qquad (10)$$

then:

$$C_D = \frac{D}{qA} = \frac{F_x}{qA} = \int_0^{\pi}\left[\frac{p(\frac{\pi}{2}-\theta)}{q}\cos\theta + \frac{\tau(\frac{\pi}{2}-\theta)}{q}\sin\theta\right]d\theta \qquad (11)$$

and $C_L = 0$ (11)

This checks exactly with the results obtained by Ashley (Ref. 5 and 6). Figure 1 is the graph of C_D versus M_∞ for $\alpha = 0^o$ and $\alpha = 45^o$. Figure 1 (a) is a plot of C_L versus M_∞ for $\alpha = 45^o$.

2. <u>Semi-infinite right circular cone, semi-vertex angle θ, at angle of attack α.</u> Reaction at origin not included in this discussion.

$$G(x, y, z) = -x^2 \tan^2\theta + y^2 + z^2 = 0$$

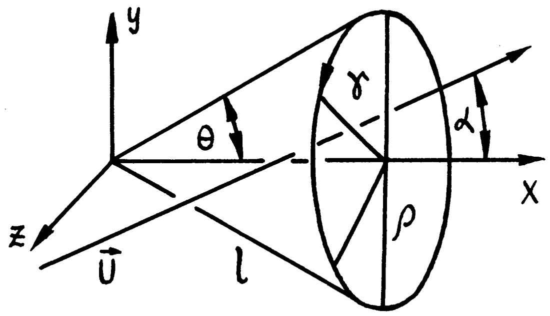

Parametric representation:

$x = x$
$y = x \tan\theta \cos\gamma$
$z = x \tan\theta \sin\gamma$
$\rho = \sqrt{y^2 + x^2} = x \tan\theta$ (1)

$$G_x = -2x \tan^2\theta, \quad G_y = 2y, \quad G_z = 2z$$

$$\Gamma_x = \sin\theta, \quad \Gamma_y = -\cos\theta\cos\gamma, \quad \Gamma_z = -\cos\theta\sin\gamma \tag{2}$$

U is parallel to x- y- plane; direction cosines are: cos α, sin α, 0.

$$\cos\beta = \sin\theta\cos\alpha - \sin\alpha\cos\theta\cos\gamma \tag{3}$$

$$\frac{dS}{A} = \frac{l\rho\, d\gamma}{2\pi\rho^2} = \frac{d\gamma}{2\pi\sin\theta} \tag{4}$$

$$\left.\begin{aligned} T_x &= \frac{\cos\alpha - \sin\theta\cos\beta}{\sin\beta} \\ T_y &= \frac{\sin^2\beta + \cos\beta\sin\theta\cos\alpha - \cos^2\alpha}{\sin\alpha\sin\beta} \\ T_z &= \frac{\cos\beta\sin\gamma\cos\theta}{\sin\beta} \end{aligned}\right\} \tag{5}$$

Then:

$$F_x = \frac{qA}{\pi}\int_0^{\pi}\left[\frac{p(\frac{\pi}{2}-\beta)}{q} + \frac{\tau(\frac{\pi}{2}-\beta)}{q}\left(\frac{\cos\alpha}{\sin\beta\sin\theta} - \cot\beta\right)\right]d\gamma \qquad (6)$$

$$F_y = \frac{qA}{\pi\sin\theta}\int_0^{\pi}\left[\frac{-p(\frac{\pi}{2}-\beta)}{q}\cos\theta\cos\gamma + \frac{\tau(\frac{\pi}{2}-\beta)}{q}\left(\frac{\sin^2\beta+\cos\beta\sin\theta\cos\alpha-\cos^2\alpha}{\sin\alpha\sin\beta}\right)\right]d\gamma \qquad (7)$$

$F = \sqrt{F_x^2+F_y^2}$ at $\phi = \arctan\frac{F_y}{F_x}$ in the x- y-plane

$$C_D = \frac{D}{qA} = \frac{F}{qA}\cos(\phi-\alpha)$$

$$C_L = \frac{L}{qA} = \frac{F}{qA}\sin(\phi-\alpha) \qquad (8)$$

at $\alpha = 0$,

then: $\cos\beta = \sin\theta$, $\theta = \frac{\pi}{2} - \beta$ (9)

$$T_x = \frac{1-\sin^2\theta}{\cos\theta} = \cos\theta = \sin\beta,\ T_y = \frac{\cos^2\theta+\sin^2\theta-1}{\cos\theta} = 0,\ T_z = \sin\theta\sin\gamma \qquad (10)$$

Then:

$$C_D = \frac{D}{qA} = \frac{F}{qA} = \frac{p(\theta)}{q} + \frac{\tau(\theta)}{q}\frac{\cos\theta}{\sin\theta} \qquad (11)$$

and $C_L = 0$ (11)

This is in perfect agreement with the results obtained by Ashley (Ref. 5 and 6). Figure 2 shows a graph of C_D versus M_∞ for $\alpha = 0^o$ and $\alpha = 45^o$ when $\theta = 10^o$. Figure 2 (a) is a graph of C_L versus M_∞ for $\alpha = 45^o$.

It should be noted here that although the treatment has been developed for a semi-infinite cone; the results apply also in the case of a finite cone, if one assumes the contribution of the base of the cone to be negligible.

3. Double-ogive, semi-vertex angle θ, at angle of attack α (see Appendix A).

$$G(x,y,z) = x^2 + 2\sqrt{R^2 - x^2}\, R\cos\theta + y^2 + z^2 - R^2(1+\cos^2\theta) = 0$$

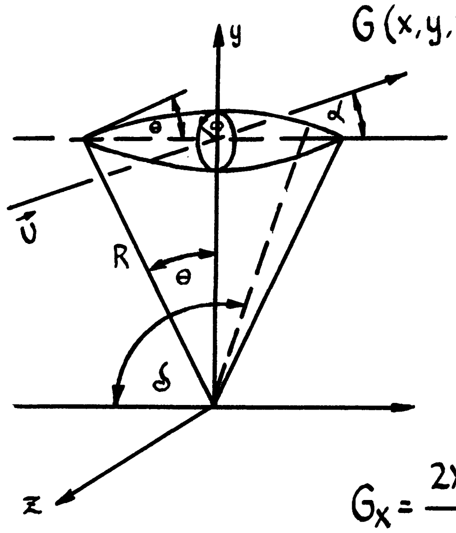

Parametric representation:

$$x = -R\cos\delta$$
$$y = R(\sin\delta - \cos\theta)\cos\phi$$
$$z = R(\sin\delta - \cos\theta)\sin\phi$$
$$\rho = R(\sin\delta - \cos\theta) = \sqrt{y^2 + z^2}$$

(1)

$$G_x = \frac{2x(\sqrt{R^2 - x^2} - R\cos\theta)}{\sqrt{R^2 - x^2}}, \quad G_y = 2y, \quad G_z = 2z \qquad (2)$$

$$\Gamma_x = \cos\delta, \quad \Gamma_y = -\sin\delta\cos\phi, \quad \Gamma_z = -\sin\delta\sin\phi$$

U is parallel to x- y- plane; direction cosines are: cos α, sin α, 0.

$$\cos\beta = \cos\delta\cos\alpha - \sin\delta\sin\alpha\cos\phi \qquad (3)$$

$$\frac{dS}{A} = \frac{R\,d\delta\, y\, d\phi}{\pi\rho^2_{(x=0)}} = \frac{(\sin\delta - \cos\theta)\cos\phi\, d\phi\, d\delta}{\pi(1-\cos\theta)^2} \qquad (4)$$

$$\left.\begin{aligned} T_x &= \frac{\cos\alpha - \cos\beta\cos\delta}{\sin\beta} \\ T_y &= \frac{\sin^2\beta + \cos\alpha\cos\beta\cos\delta - \cos^2\alpha}{\sin\beta\sin\alpha} \\ T_z &= \sin\phi\sin\delta\,\frac{\cos\beta}{\sin\beta} \end{aligned}\right\} \qquad (5)$$

Then:

$$F_x = \frac{2qA}{\pi(1-\cos\theta)^2}\int_{\frac{\pi}{2}-\theta}^{\frac{\pi}{2}+\theta} d\delta \int_0^{\pi}\left[\frac{p(\frac{\pi}{2}-\beta)}{q}\cos\delta + \frac{\tau(\frac{\pi}{2}-\beta)}{q}\,\frac{\cos\alpha - \cos\beta\cos\delta}{\sin\beta}\right]\cos\phi(\sin\delta - \cos\theta)\,d\phi$$

(6)

Similarly,

$$F_y = \frac{2qA}{\pi(1-\cos\theta)^2}\int_{\frac{\pi}{2}-\theta}^{\frac{\pi}{2}+\theta} d\delta \int_0^{\pi}\left[-\frac{p(\frac{\pi}{2}-\beta}{q}\sin\delta\cos\phi + \right.$$

(7)

$$\left.\frac{\tau(\frac{\pi}{2}-\beta)}{q}\,\frac{\sin^2\beta + \cos\alpha\cos\beta\cos\delta - \cos^2\alpha}{\sin\alpha\sin\beta}\right]\cos\phi(\sin\delta - \cos\theta)\,d\phi$$

$$F = \sqrt{F_x^2 + F_y^2} \text{ at } \phi = \arctan \frac{F_y}{F_x} \text{ in the } x, y \text{ plane} \tag{8}$$

$$C_D = \frac{D}{qA} = \frac{F}{qA} \cos(\phi - \alpha), \qquad C_L = \frac{L}{qA} = \frac{F}{qA} \sin(\phi - \alpha)$$

at $\alpha = 0$,

$$\cos\beta = \cos\delta, \; \beta = \delta, \; d\beta = d\delta, \; \frac{dS}{A} = \frac{2(\sin\beta - \cos\theta)\,d\beta}{(1 - \cos\theta)^2} \tag{9}$$

$$T_x = -\sin\beta, \quad T_y = 0, \quad T_z = \sin\phi\cos\beta \tag{10}$$

Then:

$$C_D = \frac{F_x}{qA} = \frac{2}{(1-\cos\theta)^2} \int_{\frac{\pi}{2}-\theta}^{\frac{\pi}{2}+\theta} \left[\frac{p(\frac{\pi}{2}-\beta)}{q} \cos\beta + \frac{\tau(\frac{\pi}{2}-\beta)}{q} \sin\beta \right] (\sin\beta - \cos\theta)\,d\beta \tag{11}$$

and $C_L = 0$

which checks exactly with the results obtained by Ashley (Ref. 5 and 6). Figure 3 shows a graph of C_D versus M_∞ for $\alpha = 0$ and for $\alpha = 45^o$, when $\theta = 10^o$. Figure 3 (a) is a graph of C_L versus M_∞ for $\alpha = 45^o$.

A special case of the double ogive, for $\theta = \frac{\pi}{2}$, is the sphere. Then $G(x, y, z) = x^2 + y^2 + z^2 - R^2 = 0$.

Parametric representation:

$x = -R\cos\delta$

$$G_x = 2x, \; G_y = 2y, \; G_z = 2z, \; \Gamma = 2R$$

$y = R\sin\delta\cos\phi$

$$z = R \sin\delta \sin\phi \qquad T_x = \cos\delta,\ T_y = -\sin\delta\cos\phi,\ T_z = -\sin\delta\sin\phi \qquad (2)$$

$$\rho = R \sin\delta = \sqrt{y^2 + z^2} \qquad (1)$$

Since the drag on a sphere is independent of α, let us take $\alpha = 0$. Then the direction cosines of U are $\pm 1, 0, 0$

$$\cos\beta = \cos\delta,\ \beta = \delta,\ d\delta = d\beta,\ \frac{dS}{A} = \frac{2\pi\sin\beta}{\pi}d\beta = 2\sin\beta\, d\beta \qquad (3a)$$

(4a)

$$T_x = \sin\beta, \qquad T_y = 0$$

Then:

$$\frac{F_x}{qA} = 2\int_0^{\pi}\left[\frac{p(\frac{\pi}{2}-\beta)}{q}\cos\beta\sin\beta + \frac{\tau(\frac{\pi}{2}-\beta)}{q}\sin^2\beta\right]d\beta = C_D\ \text{(sphere)}$$

(5a)

since $\frac{F_y}{qA} = 0$ by symmetry. This is identical with the result arrived at for the sphere by Ashley (Ref. 5 and 6).

4. Prolate ellipsoid of revolution, at angle of attack

$$G(x,y,z) = \frac{x^2}{a^2} + \frac{y^2+z^2}{b^2} - 1 = 0$$

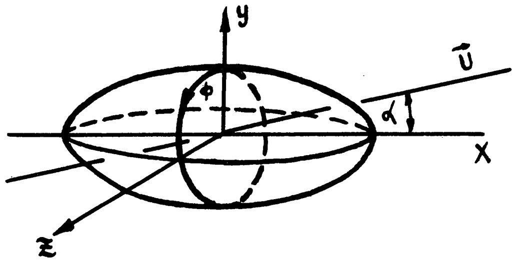

Parametric representation:

$$x = -a\cos\theta$$
$$y = b\sin\theta\cos\phi$$
$$z = b\sin\theta\sin\phi$$
$$\rho = b\sin\theta = \sqrt{y^2 + z^2} \qquad (1)$$

$$G_x = \frac{2x}{a^2}, \quad G_y = \frac{2y}{b^2}, \quad G_z = \frac{2z}{b^2}$$

$$\Gamma_x = \frac{b\cos\theta}{aK}, \Gamma_y = -\frac{\sin\theta\cos\phi}{K}, \Gamma_z = -\frac{\sin\theta\sin\phi}{K}, K = \sqrt{\frac{b^2}{a^2}\cos^2\theta + \sin^2\theta} \tag{2}$$

U is parallel to x- y- plane; direction cosines are: cos α, sin α, 0.

$$\cos\beta = \frac{1}{K}\left(\frac{b}{a}\cos\alpha\cos\theta - \sin\alpha\sin\theta\cos\phi\right) \tag{3}$$

$$\frac{dS}{A} = \frac{\sqrt{a^2\sin^2\theta + b^2\cos^2\theta}\ \sin\theta\, d\theta\, d\phi}{\pi b}$$

$$= \frac{K\sin\theta\, d\theta\, d\phi}{\pi\cdot\frac{b}{a}} \tag{4}$$

$$T_x = \frac{\cos\alpha - \frac{b}{aK}\cos\theta\cos\beta}{\sin\beta}$$

$$T_y = \frac{\sin^2\beta + \frac{b}{aK}\cos\alpha\cos\beta\cos\theta - \cos^2\alpha}{\sin\beta\sin\alpha} \tag{5}$$

$$T_z = \frac{\sin\theta\sin\phi\cos\beta}{K\sin\beta}$$

Then:

$$F_x = \frac{2qA}{\pi}\int_{\phi=0}^{\pi}\int_{\theta=0}^{\pi}\left[\frac{p(\frac{\pi}{2}-\beta)}{q}\sin\theta\cos\theta + \frac{\tau(\frac{\pi}{2}-\beta)}{q}\frac{\sin\theta}{\sin\beta}\left(\cos\alpha - \frac{b}{aK}\cos\theta\cos\beta\right)\right]d\theta\, d\phi \tag{6}$$

$$F_y = \frac{2qA}{\pi}\frac{a}{b}\int_{\phi=0}^{\pi}\int_{\theta=0}^{\pi}\left[\frac{p(\frac{\pi}{2}-\beta)}{q}\sin^2\theta\cos\phi + \frac{\tau(\frac{\pi}{2}-\beta)}{q}\frac{\sin\theta}{\sin\beta\sin\alpha}(\sin^2\beta\right.$$

$$\left. + \frac{b}{aK}\cos\alpha\cos\beta\cos\theta - \cos^2\alpha)\right] d\theta\, d\phi \tag{7}$$

$$\left.\begin{aligned} &F = \sqrt{F_x^2 + F_y^2} \text{ at } \phi = \arctan\frac{F_y}{F_x} \text{ in the x,y-plane} \\ &C_D = \frac{D}{qA} = \frac{F}{qA}\cos(\phi - \alpha) \\ &C_L = \frac{L}{qA} = \frac{F}{qA}\sin(\phi - \alpha \end{aligned}\right\} \tag{8}$$

$$\text{at } \alpha = 0 \quad \frac{dS}{A} = 2\frac{a}{b}K\sin\theta\, d\theta$$

$$\cos\beta = \frac{b\cos\theta}{aK}, \quad \sin\beta = \sqrt{1-\cos^2\beta} = \frac{\sin\theta}{K} \tag{9}$$

$$\left.\begin{aligned} &T_x = \frac{\sin^2\theta}{\sin\beta\cdot K^2} = \frac{\sin\theta}{K} = \sin\beta \\ &T_y = 0 \end{aligned}\right\} \tag{10}$$

$$\text{Then } C_D = \frac{D}{qA} = \frac{F_x}{qA} = 2\int_0^{\pi}\left[\frac{p(\frac{\pi}{2}-\beta)}{q}\sin\theta\cos\theta + \frac{\tau(\frac{\pi}{2}-\beta)}{q}\frac{a}{b}\sin^2\theta\right] d\theta \text{ and } C_L = 0 \tag{11}$$

This result may, if desired, be expressed solely in terms of β, by replacing the θ terms by their equivalent β terms:

example:
$$\sin\theta = \frac{b}{c}\,\frac{\sin\beta}{\sqrt{\frac{a^2}{c^2} - \sin^2\beta}}$$

where: $c^2 = a^2 - b^2$ (12)

A graph of C_D versus M_∞ for $\alpha = 0^o$ and 45^o where the ratio of minor axis to major axis is: $\frac{b}{a} = 0.09475$ appears in figure 4. Figure 4 (a) is a graph of C_L versus M_∞ for $\alpha = 45^o$.

A special case of the ellipsoid, for a = b (= R), is the sphere. Then $G(x, y, z) = x^2 + y^2 + z^2 - R^2 = 0$, $K = 1$ and (11) becomes

$$C_D = \frac{D}{qA} = \frac{F_x}{qA} = 2\int_0^\pi \left[\frac{p(\frac{\pi}{2}-\theta)\sin\theta\cos\theta}{q} + \frac{\tau(\frac{\pi}{2}-\theta)\sin^2\theta}{q}\right] d\theta \tag{6a}$$

which is identical with that obtained by similar means with the double ogive.

5. Body formed by joining an ogive of vertex angle 10^o and a semi-ellopsoid with $\frac{b}{a} = 0.09475$ at α angle of attack.

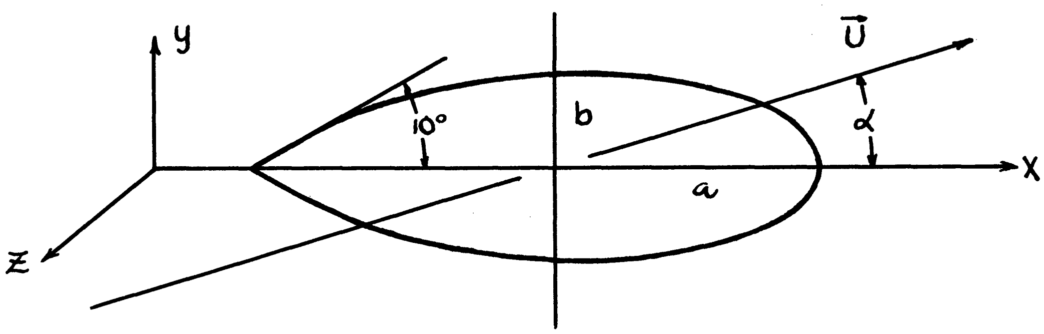

At angle of attack α, the restoring force on this body (let us call it M_I) may be determined by adding the contributions of each piece separately:

$$\frac{F_x}{qA}(M_I) = \frac{F_x}{qA}(\text{ogive})\Bigg|_{\delta = 80^\circ}^{\delta = 90^\circ} + \frac{F_x}{qA}(\text{ellipsoid})\Bigg|_{\theta = \frac{\pi}{2}}^{\theta = \pi}$$

$$\frac{F_y}{qA}(M_I) = \frac{F_y}{qA}(\text{ogive})\Bigg|_{\delta = 80^\circ}^{\delta = 90^\circ} + \frac{F_y}{qA}(\text{ellipsoid})\Bigg|_{\theta = \frac{\pi}{2}}^{\theta = \pi}$$

where each of the pressure components is based on the area of the circle of intersection of the ellipsoid with the ogive.

Then, as before, $\frac{F}{qA} = \sqrt{\left(\frac{F_x}{qA}\right)^2 + \left(\frac{F_y}{qA}\right)^2}$ at angle $\phi = \arctan \frac{F_y}{F_x}$.

$$C_D = \frac{F}{qA}\cos(\phi - \alpha)$$

$$C_L = \frac{F}{qA}\sin(\phi - \alpha)$$

at $\alpha = 0$, $C_L = 0$, and C_D is simply $\frac{F_x}{qA}$

Figure 5 shows a graph of C_D versus M_∞ for $\alpha = 0$ and for $\alpha = 45^\circ$, for M_I . Figure 5 (a) is a graph of C_L versus M_∞ for $\alpha = 45^\circ$.

IV. TYPICAL NUMERICAL CALCULATIONS

As mentioned earlier, the calculations performed to obtain the results plotted on the graphs of this report generally involve numerical integration. A typical group of such calculations is included here.

Since the drag "law" changes as M_∞ decreases through and beyond unity, there is some doubt as to the validity of the results listed for $M_\infty < 1$. However, since such experimental data as do exist agree qualitatively, at least down to $M_\infty = 0.5$, with these results, we have included them in this paper.

A. NORMAL AND SHEAR STRESSES

As cited above, the method used in obtaining aerodynamic coefficients at angle of attack was developed on the basis of the expressions for pressure (normal and tangential) on the body in flight.

These expressions, derived in Section II are:

$$\frac{p_i(\theta)}{q} = \sin\theta \, \frac{e^{-M_\infty^2 \sin^2\theta}}{M_\infty\sqrt{\pi}} + \left[1 + \operatorname{erf}(M_\infty \sin\theta)\right]\left(\frac{1 + 2M_\infty^2\sin^2\theta}{2M_\infty^2}\right) \qquad (1)$$

$$\frac{\tau_i(\theta)}{q} = \cos\theta\left\{\frac{e^{-M_\infty^2\sin^2\theta}}{M_\infty\sqrt{\pi}} + \sin\theta\left[1 + \operatorname{erf}(M_\infty\sin\theta)\right]\right\} \qquad (2)$$

$$\frac{p_r(\theta)}{q} = \frac{c_r}{c_i}\,\frac{\sqrt{\pi}}{2M_\infty}\left\{\frac{e^{-M_\infty^2\sin^2\theta}}{M_\infty\sqrt{\pi}} + \sin\theta\left[1 + \operatorname{erf}(M_\infty\sin\theta)\right]\right\} \qquad (3)$$

where the total normal pressure is:

$$\frac{p(\theta)}{q} = \frac{p_i(\theta)}{q} + \frac{p_r(\theta)}{q} \qquad (4)$$

and the total tangential stress is:

$$\frac{\tau(\theta)}{q} = \frac{\tau_i(\theta)}{q} \qquad (5)$$

In every application so far considered (requiring numerical integration), the tangential stress term contained a factor of:

$$\frac{\tau\left(\frac{\pi}{2} - \beta\right)}{q}$$

which is equivalent to:

$$\frac{\tau(\theta)}{q \cos\theta}$$

So, instead of (2), tabulation was made of:

$$\frac{\tau(\theta)}{q \cos\theta} = \frac{e^{-M_\infty^2 \sin^2\theta}}{M_\infty \sqrt{\pi}} + \sin\theta\left[1 + \mathrm{erf}(M_\infty \sin\theta)\right] \qquad (2a)$$

It must be remembered that $\frac{\tau}{q} \equiv 0$, for $\theta = \pm\frac{\pi}{2}$. However, values of $\frac{\tau(\theta)}{q \cos\theta}$ have been tabulated for $\theta = \pm\frac{\pi}{2}$ for purposes of interpolation.

In these calculations we were concerned with bracketing all values of lift and drag coefficients believed possible. Thus, the lower bound is that for the reflection mechanism of uniform adsorbed layer, in which case:

$\frac{pr(\theta)}{q} = 0$. The upper bound is that for "extreme" diffuse reflection, in which case: $\frac{c_r}{c_i} = 1$. To prepare for all other cases, $0 < \frac{c_r}{c_i} < 1$, tabulation was made of:

$$\frac{1}{\frac{c_r}{c_i}} \cdot \frac{p_r(\theta)}{q} = \frac{\sqrt{\pi}}{2M_\infty}\left\{\frac{e^{-M_\infty^2 \sin^2\theta}}{M_\infty\sqrt{\pi}} + \sin\theta\left[1+\operatorname{erf}(M_\infty \sin\theta)\right]\right\} \qquad (3a)$$

A typical calculation of:

$\frac{p_i(\theta)}{q}$, $\frac{\tau_i(\theta)}{q\cos\theta}$, $\frac{1}{c_r/c_i} \cdot \frac{p_r(\theta)}{q}$ at $= 22^\circ 30'$ and the tabulation of the results of all other such calculations performed to date by the author are presented in Tables 1, 2, 3, and 4.

B. METHOD OF NUMERICAL INTEGRATION

The method used for numerically integrating was Simpson's parabolic rule:

If the integral we evaluate is $y = \int_0^{\frac{\pi}{2}} F(M,\theta)\, d\theta \qquad (1)$

we divide the interval from 0 to $\frac{\pi}{2}$ into an even number (= n) of parts, each equal to $\Delta\theta$.

Applying Simpson's rule, taking n equal to 4,

$$y \cong \frac{\Delta\theta}{3}\left[F(M,\theta_0) + 4F(M,\theta_0+\Delta\theta) + 2F(M,\theta_0+2\Delta\theta) + 4F(M,\theta_0+3\Delta\theta) + F(M,\theta_1)\right] \qquad (2)$$

$$= \frac{1}{3} \cdot \frac{\pi}{8} \left[F(M,0) + 4F\left(M,\frac{\pi}{8}\right) + 2F\left(M,\frac{\pi}{4}\right) + 4F\left(M, \frac{3\pi}{8}\right) + F\left(M,\frac{\pi}{2}\right) \right] \tag{2a}$$

Similarly, for evaluating a double integral, such as

$$Z = \int_0^{\pi} d\phi \int_0^{\frac{\pi}{2}} F(M,\theta,\phi)\, d\theta \tag{3}$$

the process is merely repeated so that:

$$z = \int_0^{\pi} y.d\phi \tag{3a}$$

where $$y = \int_0^{\frac{\pi}{2}} F(M,\theta,\phi)\, d\theta \tag{1a}$$

is evaluated as before for each value of ϕ, taken as the endpoints of the equal number of parts into which the interval from 0 to π has been divided.

Then for $\Delta\theta = \frac{\pi}{8}$, $\Delta\phi = \frac{\pi}{4}$,

$$Z \cong \frac{\Delta\phi}{3} \cdot \frac{\Delta\theta}{3} \Big\{ \left[F(M,\theta_0,\phi_0) + 4F(M,\theta_0+\Delta\theta,\phi_0) + 2F(M,\theta_0+2\Delta\theta,\phi_0) + 4F(M,\theta_0+3\Delta\theta,\phi_0) + F(M,\theta,\phi_0)\right]$$

$$+4\left[F(M,\theta_0,\phi_0+\Delta\phi) + 4F(M,\theta_0+\Delta\theta,\phi_0+\Delta\phi) + 2F(M,\theta_0+2\Delta\theta,\phi_0+\Delta\phi) + 4F(M,\theta_0+3\Delta\theta,\phi_0+\Delta\phi) + F(M,\theta_1,\phi_0+\Delta\phi)\right]$$

$$+2\left[F(M,\theta_0,\phi_0+2\Delta\phi)+4F(M,\theta_0+\Delta\theta,\phi_0+2\Delta\phi)+2F(M,\theta_0+2\Delta\theta,\phi_0+2\Delta\phi)+4F(M,\theta_0+3\Delta\theta,\phi_0+2\Delta\phi)+F(M,\theta_1,\phi_0+2\Delta\phi)\right]$$

$$+4\left[F(M,\theta_0,\phi_0+3\Delta\phi)+4F(M,\theta_0+\Delta\theta,\phi_0+3\Delta\phi)+2F(M,\theta_0+2\Delta\theta,\phi_0+3\Delta\phi)+4F(M,\theta_0+3\Delta\theta,\phi_0+3\Delta\phi)+F(M,\theta_1,\phi_0+3\Delta\phi)\right]$$

$$+\left[F(M,\theta_0,\phi_1)+4F(M,\theta_0+\Delta\theta,\phi_1)+2F(M,\theta_0+2\Delta\theta,\phi_1)+4F(M,\theta_0+3\Delta\theta,\phi_1)+F(M,\theta,\phi_1)\right]\Bigg\} \quad (4)$$

C. DETERMINATION OF C_L AND C_D FOR DOUBLE OGIVE, HALF ANGLE $\theta = 10^\circ$, AT ANGLE OF ATTACK 45°

As derived in Section III C, the force components on a double ogive, of half angle 10°, at angle of attack of 45° are given by:

$$\frac{F_x}{qA} = \frac{2}{\pi(1-\cos\theta)^2}\int_{\frac{\pi}{2}-\theta}^{\frac{\pi}{2}+\theta} d\delta \int_0^{\pi}\left[\frac{p(\frac{\pi}{2}-\beta)}{q}\cos\delta + \frac{\tau(\frac{\pi}{2}-\beta)}{q\sin\beta}(\cos\alpha-\cos\beta\cos\delta)\right]\cos\phi(\sin\delta\cdot\cos\theta)\,d\phi \quad (1)$$

$$\frac{F_y}{qA} = \frac{2}{\pi(1-\cos\theta)^2}\int_{\frac{\pi}{2}-\theta}^{\frac{\pi}{2}+\theta} d\delta \int_0^{\pi}\left[\frac{p(\frac{\pi}{2}-\beta)}{q}\sin\delta\cos\phi + \frac{\tau(\frac{\pi}{2}-\beta)}{q\sin\beta}(\sin^2\beta+\cos\alpha\cos\beta\cos\delta-\cos^2\alpha)\right]$$

$$\cdot\cos\phi(\sin\delta-\cos\theta)\,d\phi \quad (2)$$

where $\cos\beta = \cos\delta\ \cos\alpha - \sin\delta\ \sin\alpha\ \cos\phi$ (3)

Then δ is to be integrated from 80° to 100°, over a range of 20°. Choosing $\Delta\delta = 10°$, we must evaluate (1) and (2) for δ = 80°, 90°, 100°.

But $\frac{F_x}{qA} \equiv 0 \equiv \frac{F_y}{qA}$ for δ = 80° and 100°, since $\cos 10° \equiv \sin 80° \equiv \sin 100°$.

Then our evaluation is limited to δ = 90°, when (1) and (2) become:

$$\frac{F_x}{qA} \cong \frac{8\cos\alpha}{\pi(0.01519)}\int_0^{\pi}\frac{\tau\left(\frac{\pi}{2}-\beta\right)}{q\sin\beta}\cos\phi\, d\phi \tag{1a}$$

$$\frac{F_y}{qA} \cong \frac{8}{\pi(0.01519)}\int_0^{\pi}\left[\frac{p\left(\frac{\pi}{2}-\beta\right)}{q}\cos\phi + \frac{\tau\left(\frac{\pi}{2}-\beta\right)}{q\sin\beta}\left(\frac{\sin^2\beta-\cos^2\alpha}{\sin\alpha}\right)\right]\cos\phi\, d\phi \tag{2a}$$

Taking $\Delta\phi$ = 30°, we must evaluate (1a) and (2a) for ϕ = 0°, 30°, 60°, 90°, 120°, 150°, and 180°.

Since $\cos 90° \equiv 0$, we need not evaluate for ϕ = 90°. First we must determine β for ϕ = 0°, 30°, 60°, 120°, 150°, and 180°. To do this, we complete the following table:

$\cos\beta = -0.70711\ \cos\phi$, taking $\alpha = 45°$

ϕ	0°	30°	60°	90°	120°	150°	180°
$\cos\phi$	1	0.86603	0.5	0	- 0.5	- 0.86603	- 1
$\cos\beta$	- 0.70711	- 0.61238	- 0.35356	0	+ 0.35356	+ 0.61238	+ 0.70711
β	135°	127.76°	110.7°	90°	69.3°	52.24°	45°
$\frac{\pi}{2} - \beta$	- 45°	- 37.76°	- 20.7°	0°	+ 20.7°	+ 37.76°	+ 45°

Then we evaluate (1a) as follows:

$$\frac{F_x}{qA} \cong \frac{8.070711}{\pi(0.01591)} \frac{\pi}{18} \frac{1}{3} \frac{\pi}{6} \frac{1}{3} \left[\frac{\tau(45^\circ)}{q\cos 45^\circ} + 3.46412 \frac{\tau(31.76^\circ)}{q\cos 37.76^\circ} + \frac{\tau(20.7)^\circ}{q\cos 20.7^\circ} - \frac{\tau(-20.7)^\circ}{q\cos 20.7^\circ} - 3.46412 \frac{\tau(-37.76)^\circ}{q\cos 37.76^\circ} - \frac{\tau(-45^\circ)}{q\cos 45^\circ} \right]$$

$$\cong \frac{0.70711}{243} \cdot \frac{2\pi}{0.01519} \left[\frac{\tau(45^\circ) - \tau(-45^\circ)}{q\cos 45^\circ} + 3.46412 \frac{\tau(37.76^\circ) - \tau(-37.76^\circ)}{q\cos(37.76^\circ)} + \frac{\tau(20.7^\circ) - \tau(-20.7^\circ)}{q\cos 20.7^\circ} \right]$$

(1b)

Ordinarily a table must be set up in which the values of each of the stresses occurring in such an equation is listed for each M_∞ desired (see below, as was done for (2b)). However, in the case of (1b), the stresses are independent of M_∞, i.e., they are constant. When the values are read or interpolated from Table 1 it is a simple matter to calculate:

$$\frac{F_x}{qA} \cong 7.66 \qquad (1c)$$

for this configuration for all M_∞ .

If a better approximation had been determined, e.g., by taking $\Delta\delta = 5^\circ$, it is likely that $\frac{F_x}{qA}$ would not have been exactly constant. This is purely a result of the fact that the approximation first determined was found by computation for a single δ , namely, $\delta = 90^\circ$. However, when better approximation was calculated, the variation in value of $\frac{F_x}{qA}$ with M_∞ was so small that the additional work entailed produced no appreciable difference in the final evaluation of the drag and lift coefficients.

Evaluation of (2a) is as follows:

$$\frac{F_y}{qA} \cong \frac{8}{\pi(0.01519} \, \frac{\pi}{18} \, \frac{1}{3} \, \frac{\pi}{6} \, \frac{1}{3} \left\{ \frac{p(45^\circ)+p(-45^\circ)}{q} + 3\,\frac{p(37.76^\circ)+p(-37.76^\circ)}{q} + 0.5\,\frac{p(20.7^\circ)+p(-20.7^\circ)}{q} + 0.70711\left[0.86603\,\frac{\tau(37.76^\circ)-\tau(-37.76^\circ)}{q\cos(37.76^\circ)} + 0.75\,\frac{\tau(20.7^\circ)-\tau(20.7^\circ)}{q\cos(20.7^\circ)}\right] \right\} \qquad (2b)$$

The steps and tabulation involved in evaluating (2b) and then determining C_D and C_L by proper manipulation of (1c) and (2b) are shown in Tables 5 and 6.

In like manner, the coefficients for the semi-infinite right circular cone, infinite right circular cylinder, and prolate ellipsoid at an angle of attack of 45° were obtained. The results are presented in Table 7.

D. M_I AT ANGLE OF ATTACK OF 45°

As discussed earlier, the M_I consists of half of a double ogive plus half of a prolate ellipsoid. The restoring force on the M_I, at any angle of attack α, may be determined by adding the contributions of each piece separately:

$$\frac{F_x}{qA}(M_I) = \frac{F_x}{qA}(\text{ogive})\Bigg|_{\delta=80^\circ}^{\delta=90^\circ} + \frac{F_x}{qA}(\text{ellipsoid})\Bigg|_{\theta=\frac{\pi}{2}}^{\theta=\pi}$$

$$\frac{F_y}{qA}(M_I) = \frac{F_y}{qA}(\text{ogive})\Bigg|_{\delta=80^\circ}^{\delta=90^\circ} + \frac{F_y}{qA}(\text{ellipsoid})\Bigg|_{\theta=\frac{\pi}{2}}^{\theta=\pi}$$

By the methods of part IV B above, the following table containing the contribution of each piece was completed and the coefficients obtained (see Table 8).

REFERENCES

I. Free Molecule Flow

1. Zahm, A. F., "Superaerodynamics", Journal of the Franklin Institute, Vol. 217, pp. 153-166, 1934.

2. Sänger, E., "Gaskinetik Sehr Hoher Fluggeschwindigkeiten", Deutsche Luftfahrtforschung, Bericht 972, Berlin 1938. Translated by Liebkold, 1946, for Douglas Aircraft.

3. Snow, R. M., "Aerodynamics of Ultra-High Altitude Missiles", APL/JHU-CM-498, September 1948.

4. Tsien, H. S., "Superaerodynamics, Mechanics of Rarefied Gases", Journal of the Aeronautical Sciences, Vol. 13, No. 12, pp. 653-664, December 1946.

5. Ashely, H., "Applications of the Theory of Free Molecule Flow to Aeronautics", Journal of the Aeronautical Sciences, Vol. 16, No. 2, pp. 95-104, February 1949.

6. Ashley, H., "Applications of the Theory of Free Molecule Flow to Aeronautics", IAS Preprint No. 164.

II. General

7. Schultz, F. V., Spencer, N. W., and Reifman, A., "Upper Air Research Program", Report No. 2, ERI, University of Michigan, 1 July 1948.

8. Grimminger, G., "Analysis of Temperature, Pressure and Density of the Atmosphere Extending to Extreme Altitudes", Rand R-105, 1 November 1948.

9. Weidman, M. L., "Thermal Accommodation Coefficient", Transections of ASME, Vol. 68, pp. 57-64, 1946.

REFERENCES (CONTINUED)

10. Millikan, R. A., "Coefficients of Slip in Gases and the Law of Reflection of Molecules from the Surfaces of Solids and Liquids", Physical Review, Vol. 21, pp. 217-238, 1923.

11. Kennard, E. H., "Kinetic Theory of Gases", McGraw-Hill Book Co., Inc., New York, 1936.

APPENDIX A

Note on the Double Ogive

A double ogive is formed by rotating the arc of a circle about its chord (see below). The vertex angle (2θ) of the ogive is then equal to the central angle of the generating arc (generatrix).

δ is defined as the angle between the negative x-axis and a normal to the generatrix.

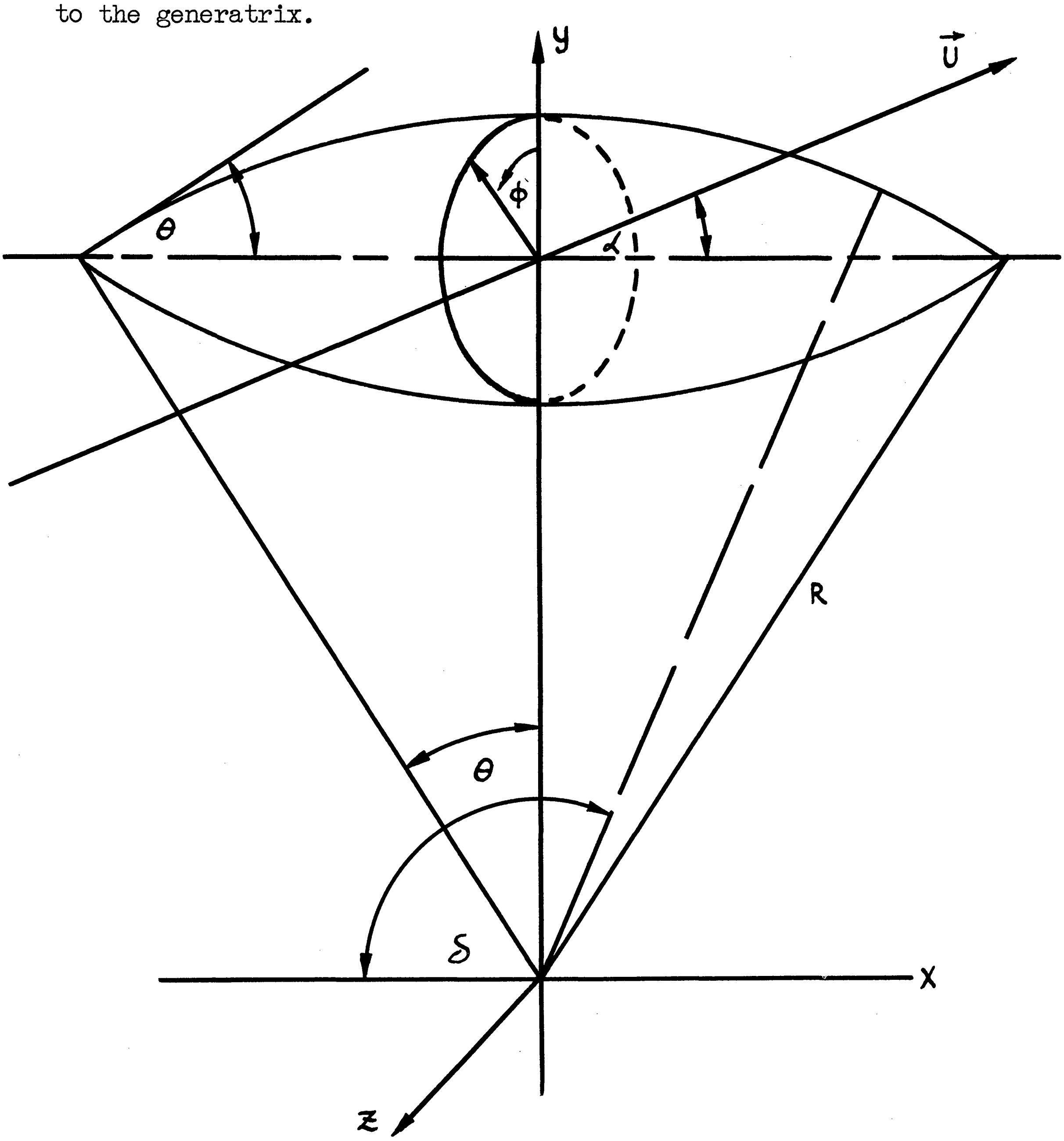

APPENDIX B

TABLES

FIGURES

FIGURES (CONT'D)

TABLE 1

Determination of $\frac{p_i(\theta)}{q}$, $\frac{1}{\left(\frac{c_r}{c_i}\right)} \cdot \frac{p_r(\theta)}{q}$, $\frac{\tau_i(\theta)}{q \cos \theta}$ For $\theta = 22^\circ\ 30'$

Step	Operation \ M_∞	0.4	0.5	0.6	0.8	1.0	1.2	1.5	2.0	4.0	7.0	10.0
(1)	$M_\infty \sin$	0.1531	0.1913	0.2296	0.3061	0.3827	0.4592	0.5740	0.7654	1.5307	2.6788	3.8268
(2)	$M_\infty^2 \sin^2\theta$	0.0234	0.0366	0.0527	0.0937	0.1464	0.2109	0.3295	0.5858	2.3431	7.1758	14.6444
(3)	$e^{-(2)}$	0.9867	0.9641	0.9487	0.9105	0.8638	0.8099	0.7193	0.5567	0.0960	0.0009	0 —
(4)	$\frac{1}{M_\infty\sqrt{\pi}}$	1.4105	1.1284	0.9403	0.7052	0.5642	0.4702	0.3761	0.2821	0.1410	0.0806	0.0564
(5)	(3) × (4)	1.3917	1.0878	0.8920	0.6421	0.4873	0.3808	0.2705	0.1570	0.0135	0.0001	0 —
(6)	(5) × sin θ	0.5326	0.4163	0.3414	0.2457	0.1865	0.1457	0.1035	0.0601	0.0052	0 —	0 —
(7)	1+erf (1)	1.1714	1.2132	1.2546	1.3292	1.4116	1.4840	1.5831	1.7209	1.9696	1.9998	2 —
(8)	1-erf (1)	0.8286	0.7868	0.7454	0.6708	0.5884	0.5160	0.4169	0.2791	0.0304	0.0002	0 —
(9)	$\frac{0.5 + (2)}{M_\infty^2}$	3.2713	2.1464	1.5353	0.9277	0.6464	0.4937	0.3687	0.2714	0.1777	0.1566	0.1514
(10)	(7) × (9)	3.8320	2.6041	1.9262	1.2331	0.9125	0.7326	0.5836	0.4671	0.3500	0.3133	0.3029
(11)	(8) × (9)	2.7106	1.6888	1.1444	0.6223	0.3804	0.2547	0.1537	0.0758	0.0054	0 —	0 —
$\frac{p_i}{q}\theta$	(10) + (6)	4.3646	3.0204	2.2676	1.4788	1.0990	0.8783	0.6872	0.5272	0.3552	0.3133	0.3029
$\frac{p_i(-\theta)}{q}$	(11) - (6)	2.1780	1.2725	0.8031	0.3766	0.1939	0.1090	0.0502	0.0157	0.0002	0 —	0 —
(12)	(7) × sin θ	0.4483	0.4643	0.4701	0.4987	0.5302	0.5579	0.5958	0.6486	0.7537	0.7653	0.7654
(13)	(8) × sin θ	0.3171	0.3011	0.2852	0.2567	0.2252	0.1975	0.1595	0.1068	0.0116	0 —	0 —
$\frac{\tau(\theta)}{q \cos \theta}$	(5)+(12)= (14)	1.8400	1.5521	1.3621	1.1408	1.0175	0.9387	0.8664	0.8056	0.7673	0.7654	0.7654

TABLE 1

Determination of $\frac{p_i(\theta)}{q}$, $\frac{1}{\left(\frac{c_r}{c_i}\right)} \cdot \frac{p_r(\theta)}{q}$, $\frac{\tau_i(\theta)}{q \cos \theta}$ For θ = 22° 30'

(Continued)

Step	Operation \ M_∞	0.4	0.5	0.6	0.8	1.0	1.2	1.5	2.0	4.0	7.0	10.0
$\frac{\tau(-\theta)}{q \cos \theta}$	(5)-(13)=(15)	1.0746	0.7867	0.6068	0.3854	0.2622	0.1833	0.1110	0.0502	0.0019	0 —	0 —
(16)	$\frac{\sqrt{\pi}}{2M_\infty}$	2.2156	1.7725	1.4770	1.1078	0.8862	0.7385	0.5908	0.4431	0.2216	0.1266	0.0886
$\frac{1}{\frac{c_v}{c_i}} \frac{p_r(\theta)}{q}$	(14)×(16)	4.0766	2.7510	2.0119	1.2638	0.9017	0.6933	0.5119	0.3570	0.1700	0.0969	0.0678
$\frac{1}{\frac{c_v}{c_i}} \frac{p_r(-\theta)}{q}$	(15)×(16)	2.3809	1.3944	0.8962	0.4270	0.2323	0.1354	0.0656	0.0223	0.0042	0 —	0 —

TABLE 2

$\frac{p_1(\theta)}{q}$

θ \ M_∞	0.4	0.5	0.6	0.8	1.0	1.2	1.5	2.0	4.0	7.0	10.0
-90°	1.1559	0.5597	0.2902	0.0875	0.0284	0.0095	0.0018	0.0001	0.—	0.—	0.—
-60°	1.3355	0.6764	0.3674	0.1231	0.0451	0.0172	0.0041	0.0003	0.—	0.—	0.—
-45°	1.5719	0.8386	0.4807	0.1808	0.0753	0.0331	0.0102	0.0014	0.—	0.—	0.—
-40.8°	1.6672	0.9005	0.5252	0.2050	0.0890	0.0410	0.0145	0.0022	0.—	0.—	0.—
-37.76°	1.7384	0.9502	0.5611	0.2250	0.1007	0.0480	0.0167	0.0031	0.—	0.—	0.—
-30°	1.9458	1.0983	0.6707	0.2890	0.1400	0.0726	0.0292	0.0071	0.—	0.—	0.—
-22.5°	2.1781	1.2725	0.8031	0.3766	0.1939	0.1090	0.0502	0.0157	0.0002	0.—	0.—
-20.7°	2.2461	1.3189	0.8391	0.3943	0.2096	0.1202	0.0570	0.0188	0.0004	0.—	0.—
-15.7°	2.4320	1.4590	0.9488	0.4670	0.2620	0.1572	0.0810	0.0310	0.0013	0.—	0.—
-10°	2.6644	1.6373	1.0912	0.5650	0.3324	0.2117	0.1188	0.0533	0.0049	0.0003	0.—
-5°	2.8867	1.8110	1.2324	0.6658	0.4090	0.2726	0.1640	0.0830	0.0133	0.0021	0.0004
-3°	2.9801	1.8846	1.2932	0.7101	0.4436	0.3007	0.1855	0.0981	0.0190	0.0041	0.0013
0°	3.1250	2.0000	1.3889	0.7813	0.5000	0.3472	0.2222	0.1250	0.0313	0.0102	0.0050
3°	3.2753	2.1208	1.4900	0.8578	0.5620	0.4000	0.2644	0.1574	0.0490	0.0218	0.0142
5°	3.3785	2.2043	1.5606	0.9120	0.6062	0.4371	0.2958	0.1823	0.0644	0.0335	0.0248
10°	3.6460	2.4230	1.7470	1.0580	0.7280	0.5430	0.3860	0.2570	0.1180	0.0805	0.0703
15.7°	3.9644	2.6875	1.9755	1.2421	0.8844	0.6840	0.5100	0.3654	0.2076	0.1668	0.1582
20.7°	4.2540	2.9310	2.1890	1.4180	1.0400	0.8240	0.6380	0.4810	0.3120	0.2700	0.2600

TABLE 2

$\frac{p_i(\theta)}{q}$ (Continued)

θ \ M_∞	0.4	0.5	0.6	0.8	1.0	1.2	1.5	2.0	4.0	7.0	10.0
22.5°	4.3646	3.0204	2.2676	1.4788	1.0990	0.8783	0.6872	0.5272	0.3552	0.3133	0.3030
30°	4.8042	3.4017	2.6071	1.7735	1.3600	1.1220	0.9152	0.7430	0.5625	0.5204	0.5100
37.76°	5.2616	3.8000	2.9670	2.0875	1.6500	1.4000	1.1777	0.9970	0.8125	0.7704	0.7600
40.8°	5.4364	3.9530	3.1062	2.2112	1.7645	1.5070	1.2835	1.1014	0.9161	0.8740	0.8636
45°	5.6780	4.1614	3.2970	2.3820	1.9247	1.6613	1.4342	1.2486	1.0625	1.0204	1.0100
60°	6.4246	4.8236	3.9104	2.9394	2.4550	2.1773	1.9403	1.7500	1.5625	1.5204	1.5100
90°	7.0941	5.4403	4.4876	3.4750	2.9716	2.6850	2.4427	2.2500	2.0625	2.0204	2.0100

TABLE 3

$$\frac{1}{\frac{c_r}{c_i}} \cdot \frac{p_r(\theta)}{q}$$

θ \ M_∞	0.4	0.5	0.6	0.8	1.0	1.2	1.5	2.0	4.0	7.0	10.0
-90°	1.3965	0.7077	0.3839	0.1263	0.0446	0.0160	0.0034	0.0002	0.—	0.—	0.—
-60°	1.5739	0.8272	0.4688	0.1695	0.0668	0.0273	0.0072	0.0007	0.—	0.—	0.—
-45°	1.8051	0.9916	0.5872	0.2353	0.1044	0.0488	0.0163	0.0027	0.—	0.—	0.—
-40.8°	1.8886	1.0518	0.6320	0.2618	0.1204	0.0587	0.0202	0.0040	0.—	0.—	0.—
-37.76°	1.9538	1.0992	0.6678	0.2832	0.1330	0.0673	0.0254	0.0053	0.—	0.—	0.—
-30°	2.1414	1.2375	0.7735	0.3490	0.1770	0.0960	0.0413	0.0111	0.—	0.—	0.—
-22.5°	2.3809	1.3944	0.8962	0.4270	0.2323	0.1354	0.0656	0.0222	0.0004	0.—	0.—
-20.7°	2.4040	1.4355	0.9287	0.4513	0.2480	0.1476	0.0730	0.0260	0.0007	0.—	0.—
-15.7°	2.5620	1.5570	1.0260	0.5180	0.2914	0.1834	0.0980	0.0400	0.0021	0.—	0.—
-10°	2.7554	1.7073	1.1475	0.6040	0.3605	0.2340	0.1345	0.0628	0.0068	0.0005	0.—
-5°	2.9357	1.8493	1.2640	0.6885	0.4266	0.2866	0.1745	0.0902	0.0157	0.0015	0.0007
-3°	3.0104	1.9086	1.3130	0.7247	0.4550	0.3100	0.1927	0.1032	0.0210	0.0024	0.0017
0°	3.1250	2.0000	1.3889	0.7813	0.5000	0.3472	0.2222	0.1250	0.0313	0.0102	0.0050
3°	3.2423	2.0941	1.4676	0.8373	0.5478	0.3873	0.2545	0.1500	0.0442	0.0182	0.0110
5°	3.3220	2.1583	1.5214	0.8771	0.5788	0.4154	0.2775	0.1674	0.0543	0.0248	0.0161
10°	3.5250	2.3230	1.6605	0.9886	0.6682	0.4905	0.3400	0.2167	0.0837	0.0444	0.0308
15.7°	3.7610	2.5161	1.8250	1.1174	0.7710	0.5830	0.4177	0.2800	0.1220	0.0690	0.0480

TABLE 3

$$\frac{1}{\frac{C_r}{C_1}} \cdot \frac{p_r(\theta)}{q} \quad \text{(Continued)}$$

θ \ M∞	0.1	0.5	0.6	0.8	1.0	1.2	1.5	2.0	4.0	7.0	10.0
20.7°	3.9706	2.6890	1.9730	1.2346	0.8746	0.6690	0.4910	0.3394	0.1573	0.0895	0.0627
22.5°	4.0766	2.7510	2.0120	1.2640	0.9020	0.6933	0.5120	0.3570	0.1700	0.0970	0.0678
30°	4.3570	3.0100	2.2505	1.4570	1.0632	0.8345	0.6320	0.4542	0.2216	0.1266	0.0886
37.76°	4.6673	3.2700	2.4768	1.6400	1.2193	0.9718	0.7490	0.5480	0.2714	0.1550	0.1085
40.8°	4.7834	3.3677	2.5619	1.7092	1.2784	1.0236	0.7922	0.5829	0.2895	0.1654	0.1158
45°	4.9387	3.5000	2.6762	1.8020	1.3578	1.0933	0.8520	0.6294	0.3133	0.1790	0.1253
60°	5.4114	3.8972	3.0271	2.0883	1.6018	1.3065	1.0306	0.7682	0.3838	0.2193	0.1535
90°	5.8276	4.2526	3.3381	2.3418	1.8170	1.4930	1.1850	0.8864	0.4431	0.2532	0.1772

TABLE 4

$$\frac{\tau(\theta)}{q \cos \theta}$$

θ \ M_∞	0.4	0.5	0.6	0.8	1.0	1.2	1.5	2.0	4.0	7.0	10.0
-90°	0.6303	0.3993	0.2600	0.1140	0.0503	0.0217	0.0057	0.0005	0.—	0.—	0.—
-60°	0.7104	0.4667	0.3174	0.1530	0.0754	0.0370	0.01225	0.00167	0.—	0.—	0.—
-45°	0.8147	0.5595	0.3975	0.2124	0.1178	0.0660	0.0276	0.0061	0.—	0.—	0.—
-40.8°	0.8524	0.5934	0.4279	0.2363	0.1359	0.0795	0.0342	0.0090	0.—	0.—	0.—
-37.76°	0.8818	0.6202	0.4521	0.2557	0.1511	0.0911	0.0430	0.0119	0.—	0.—	0.—
-30°	0.9665	0.6982	0.5237	0.3152	0.1996	0.1300	0.0700	0.0251	0.0002	0.—	0.—
-22°30'	1.0746	0.7867	0.6068	0.3854	0.2622	0.1833	0.1110	0.0502	0.0019	0.—	0.—
-20.7°	1.0850	0.8100	0.6288	0.4074	0.2797	0.2000	0.1237	0.0590	0.0030	0.—	0.—
-15.7°	1.1564	0.8784	0.6944	0.4674	0.3288	0.2483	0.1659	0.0903	0.0096	0.0002	0.—
-10°	1.2437	0.9632	0.7769	0.5452	0.4067	0.3168	0.2277	0.1418	0.0305	0.0035	0.0003
-5°	1.3250	1.0434	0.8557	0.6215	0.4813	0.3881	0.2954	0.2035	0.0707	0.0217	0.0074
-3°	1.3588	0.0768	0.8889	0.6541	0.5134	0.4197	0.3261	0.2328	0.0948	0.0388	0.0189
0°	1.4105	1.1284	0.9403	0.7052	0.5642	0.4702	0.3761	0.2821	0.1410	0.0806	0.0564
3°	1.4634	1.1815	0.9934	0.7558	0.6181	0.5244	0.4308	0.3375	0.1995	0.1435	0.1236
5°	1.4994	1.2177	1.0301	0.7948	0.6556	0.5625	0.4697	0.3778	0.2450	0.1960	0.1817
10°	1.5910	1.3105	1.1242	0.8925	0.7540	0.6641	0.5750	0.4891	0.3778	0.3508	0.3476
15.7°	1.6976	1.4196	1.2356	1.0086	0.8700	0.7895	0.7071	0.6315	0.5508	0.5414	0.5412

TABLE 4

$\frac{\tau(\theta)}{q \cos \theta}$ (Continued)

θ \ M_∞	0.1	0.5	0.6	0.8	1.0	1.2	1.5	2.0	4.0	7.0	10.0
20.7°	1.7921	1.5170	1.3359	1.1145	0.9868	0.9059	0.8308	0.7660	0.7101	0.7071	0.7071
22°30'	1.8400	1.5521	1.3621	1.1408	1.0175	0.9387	0.8664	0.8056	0.7673	0.7654	0.7654
30°	1.9665	1.6982	1.5237	1.3152	1.1996	1.1300	1.0700	11.0251	1.0002	1.—	1.—
27.76°	2.1066	1.8450	1.6769	1.4804	1.3758	1.3158	1.2678	1.2367	1.2248	1.2248	1.2248
40.8°	2.1590	1.9000	1.7345	1.5429	1.4425	1.3861	1.3408	1.3155	1.3066	1.3066	1.3066
45°	2.2291	1.9738	1.8119	1.6268	1.5321	1.4804	1.4419	1.4203	1.4142	1.4142	1.4142
60°	2.4425	2.1988	2.0494	1.8851	1.8074	1.7690	1.7443	1.7337	1.7321	1.7321	1.7321
90°	2.6303	2.3993	2.2600	2.1140	2.0503	2.0217	2.0057	2.0005	2.—	2.—	2.—

TABLE 5

Determination of $\frac{F_y}{qA}$, C_D and C_L ($\frac{p_r}{q} = 0$).

Step	Operation \ M_∞	0.4	0.5	0.6	0.8	1.0	1.2	1.5	2.0	4.0	7.0	10.0
①	$\frac{F_x}{qA}$	7.6600	7.6600	7.6600	7.6600	7.6600	7.6600	7.6600	7.6600	7.6600	7.6600	7.6600
②	$\Sigma\tau$ terms in (2b)	1.1250	1.1250	1.1250	1.1250	1.1250	1.1250	1.1250	1.1250	1.1250	1.1250	1.1250
③	$\frac{p_i(45)+p_i(-45)}{q}$	7.2500	5.0000	3.7777	2.5625	2.0000	1.6944	1.4444	1.2500	1.0625	1.0204	1.0100
④	$\frac{.5p_i(20.7)+p_i(-20.7)}{q}$	3.2500	2.1250	1.5139	0.9062	0.6250	0.4722	0.3472	0.2500	0.1562	0.1352	0.1300
⑤	$\frac{3p_i(37.76)+p_i(-37.76)}{q}$	21.0000	14.2500	10.5834	6.9376	5.2501	4.3334	3.5834	3.0000	2.4376	2.3113	2.2801
⑥	②+③+④+⑤	32.6250	22.5000	17.0000	11.5314	9.0000	7.6250	6.5000	5.6250	4.7814	4.5919	4.5451
⑦	$\frac{F_y}{qA}$ = ⑥ × $\frac{\pi}{1.8456}$	55.5351	38.3000	28.9378	19.6290	15.3200	12.9795	11.0646	9.5750	8.1390	7.8164	7.7368
⑧	tan γ_o = ⑦/①	7.2500	5.0000	3.7778	2.5625	2.0000	1.6944	1.4444	1.2500	1.0625	1.0204	1.0100
⑨	γ_o	82.15°	78.7°	75.2°	68.7°	63.4°	59.45°	55.3°	51.35°	46.75°	45.6°	45.3°
⑩	$\gamma_o - \alpha$	37.15°	33.7°	30.2°	23.7°	18.4°	14.45°	10.3°	6.35°	1.57°	0.6°	0.3°
⑪	cos 10	0.7971	0.8320	0.8645	0.9158	0.9487	0.9683	0.9839	0.9939	0.9995	0.9999	1.0000
⑫	sin 10	0.6039	0.5547	0.5026	0.4016	0.3162	0.2496	0.1789	0.1104	0.0303	0.0101	0.0050
⑬	$\frac{F}{qA} = \sqrt{①^2 + ⑦^2}$	56.0609	39.0585	29.9345	21.0707	17.1283	15.0713	13.4573	12.2620	11.1767	10.9440	10.8873
C_D	⑪ × ⑬	44.686	32.499	25.879	19.296	16.249	14.594	13.240	12.187	11.172	10.943	10.887
C_L	⑫ × ⑬	33.852	21.666	15.046	8.463	5.416	3.762	2.408	1.354	0.339	0.110	0.054

TABLE 6

Determination of $\frac{F_y}{qA}$, C_D and C_L $\quad \frac{C_r}{C_i} = 1$

Step	Operation \ M_∞	0.4	0.5	0.6	0.8	1.0	1.2	1.5	2.0	4.0	7.0	10.0
(1)	$\frac{F_x}{qA}$	7.6600	7.6600	7.6600	7.6600	7.6600	7.6600	7.6600	7.6600	7.6600	7.6600	7.6600
(2)	$\Sigma\tau$ terms in (2b)	1.1250	1.1250	1.1250	1.1250	1.1250	1.1250	1.1250	1.1250	1.1250	1.1250	1.1250
(3a)	$\frac{p_i(45)+p_i(-45)}{q}$	13.9938	9.4901	7.0412	4.6000	3.4622	2.8365	2.3126	1.8821	1.3758	1.1994	1.1353
(4a)	$\frac{0.5p_i(20.7)+p_i(-20.7)}{q}$	6.4373	4.1872	2.9648	1.7492	1.1862	0.8805	0.6292	0.4328	0.2353	0.1800	0.1613
(5a)	$\frac{3p_i(37.76)+p_i(-37.76)}{q}$	36.7029	24.6125	18.0414	11.4988	8.4594	6.7976	5.4202	4.3122	3.0812	2.6790	2.5375
(6a)	(2) + (3a) + (4a) + (5a)	58.2590	39.4148	29.1724	18.9730	14.2328	11.6396	9.4870	7.7521	5.8173	5.1837	4.9591
(7a)	$\frac{F_y}{qA}$ = (6a) $\frac{\pi}{1.8456}$	99.1700	67.0928	49.6580	32.2963	24.2274	19.8132	16.1490	13.1958	9.9024	8.8238	8.4415
(8a)	$\tan\gamma_1$ = (7a) ÷ (1)	12.9465	8.7589	6.4828	4.2162	3.1628	2.5866	2.1082	1.7227	1.2930	1.1529	1.1020
(9a)	γ_1	85.6°	83.5°	81.2°	76.65°	72.45°	68.9°	64.6°	59.9°	52.3°	49.05°	47.8°
(10a)	$\gamma_1 - \alpha$	40.6°	38.5°	36.2°	31.65°	27.45°	23.9°	19.6°	14.9°	7.3°	4.05°	2.8°
(11a)	cos (10a)	0.7595	0.7827	0.8066	0.8512	0.8874	0.9145	0.9419	0.9665	0.9919	0.9975	0.9988
(12a)	sin (10a)	0.6505	0.6223	0.5910	0.5248	0.4610	0.4046	0.3358	0.2566	0.1268	0.0704	0.0485
(13a)	$\frac{F}{qA} = \sqrt{(1)^2 + (7a)^2}$	99.4653	67.5287	50.2453	33.1923	25.4095	21.2424	17.8736	15.2579	12.5193	11.6848	11.3989
C_D	(11a) × (13a)	75.5400	52.8581	40.5300	28.2536	22.5479	19.4264	16.8355	14.7472	12.4183	11.6557	11.3854
C_L	(12a) × (13a)	64.7072	42.0251	29.6975	17.4203	11.7147	8.5938	6.0027	3.9147	1.5872	0.8230	0.5525

TABLE 7

		Uniform Adsorbed Layer $c_r/c_i = 0$		"Extreme" Diffuse Reflection $c_r/c_i = 1$	
	M_∞	C_D	C_L	C_D	C_L
Infinite Right Circular Cylinder	0.4	5.49	-1.29	7.24	-3.03
	0.5	4.46	-1.02	5.85	-2.42
	0.6	3.78	-0.85	4.94	-2.01
	0.8	2.95	-0.63	3.82	-1.50
	1.0	2.47	-0.50	3.17	-1.20
	1.2	2.18	-0.41	2.76	-1.00
	1.5	1.90	-0.33	2.37	-0.79
	2.0	1.66	-0.24	2.01	-0.59
	4.0	1.41	-0.14	1.58	-0.31
	7.0	1.36	-0.11	1.46	-0.21
	10.0	1.33	-0.09	1.40	-0.16
Semi-infinite Right Circular Cone	0.4	13.46	-0.59	19.19	0.28
	0.5	10.63	0.01	14.91	0.99
	0.6	8.91	0.19	12.32	1.21
	0.8	6.91	0.30	9.34	1.27
	1.0	5.85	0.34	7.75	1.21
	1.2	5.16	0.28	6.72	1.06
	1.5	4.55	0.23	5.80	0.90
	2.0	4.05	0.17	4.98	0.70
	4.0	3.52	0.05	3.99	0.34
	7.0	3.41	0.02	3.68	0.18
	10.0	3.39	0.01	3.58	0.12

TABLE 7 (Continued)

		Uniform Adsorbed Layer $c_r/c_i = 0$		"Extreme" Diffuse Reflection $c_r/c_i = 1$	
	M_∞	C_D	C_L	C_D	C_L
Prolate Ellipsoid Ratio of Axes $= \frac{b}{a}$ $0.09475 = \frac{b}{a}$	0.4	63.94	14.84	85.17	35.66
	0.5	51.88	11.77	68.86	28.40
	0.6	43.94	9.86	58.07	23.70
	0.8	34.38	7.19	44.98	17.58
	1.0	28.97	5.67	37.41	13.92
	1.2	25.55	4.63	32.64	11.57
	1.5	22.42	3.58	28.08	9.12
	2.0	19.72	2.55	23.93	6.79
	4.0	16.95	1.19	19.08	3.27
	7.0	16.27	0.83	17.47	2.00
	10.0	16.08	0.74	16.92	1.57

TABLE 8

CONTRIBUTIONS OF EACH PART OF M_I: $x = \frac{F_x}{qA}$, $y = \frac{F_y}{qA}$

	Item	Piece		0.4	0.5	0.6	0.8	1.0	1.2	1.5	2.0	4.0	7.0	10.0
$p_r = 0$	1)	Ogive	x	3.83	3.83	3.83	3.83	3.83	3.83	3.83	3.83	3.83	3.83	3.83
	2)		y	28.60	19.75	14.87	10.44	8.16	6.76	5.78	5.05	4.34	4.17	4.13
	3)	Ellipsoid	x	13.56	11.54	10.03	8.26	7.18	6.50	5.90	5.40	5.02	4.93	4.87
	4)		y	23.31	18.69	15.68	12.02	9.93	8.58	7.32	6.20	4.96	4.65	4.57
$\frac{c_r}{c_i} = 1$	1a)	Ogive	x	3.83	3.83	3.83	3.83	3.83	3.83	3.83	3.83	3.83	3.83	3.83
	2a)		y	48.58	32.94	24.51	16.39	12.32	10.00	8.21	6.82	5.20	4.65	4.48
	3a)	Ellipsoid	x	10.30	9.44	8.55	7.40	6.60	6.05	5.59	5.20	4.92	4.87	4.85
	4a)		y	34.79	27.82	23.22	17.63	14.31	12.31	10.24	8.36	6.03	5.24	4.98

DETERMINATION OF C_D AND C_L

	Item	Piece	0.4	0.5	0.6	0.8	1.0	1.2	1.5	2.0	4.0	7.0	10.0
$p_r=0$	Σ x	1)+3)	17.39	15.37	13.86	12.09	11.01	10.33	9.73	9.23	8.85	8.76	8.70
	Σ y	2)+4)	51.91	38.44	30.55	22.46	18.09	15.34	13.10	11.25	9.30	8.82	8.70
	tan Φ	$\frac{F_y}{F_x}$	2.9850	2.5010	2.2042	1.8577	1.6431	1.4850	1.3464	1.2189	1.0508	1.0068	1.0000
	Φ		71°29'	68°12'	65°36'	61°42'	58°40'	56°3'	53°24'	50°38'	46°25'	45°12'	45°
	γ	$\Phi - \alpha$	26°29'	23°12'	20°36'	16°42'	13°40'	11°3'	8°24'	5°38'	1°25'	0°12'	0

TABLE 8 (CONTINUED)

DETERMINATION OF C_D AND C_L

	Item	Piece	0.4	0.5	0.6	0.8	1.0	1.2	1.5	2.0	4.0	7.0	10.0
$p_r=0$	$\cos\gamma$		0.8951	0.9190	0.9361	0.9578	0.9716	0.9815	0.9893	0.9952	0.9997	1.0000	1
	$\sin\gamma$		0.4459	0.3939	0.3518	0.2874	0.2364	0.1917	0.1461	0.0982	0.0247	0.0034	0
	$\frac{F}{qA}$		54.75	41.40	33.55	25.51	21.18	18.49	16.32	14.55	12.84	12.43	12.30
	C_D	$\frac{F}{qA}\cos\gamma$	49.00	38.05	31.40	24.43	20.58	18.15	16.14	14.48	12.83	12.43	12.30
	C_L	$\frac{F}{qA}\sin\gamma$	24.41	16.31	11.80	7.33	5.01	3.55	2.38	1.43	0.32	0.04	0
Similarly for $\frac{c_r}{c_i} = 1$		C_D	68.94	52.35	42.51	32.00	26.21	22.76	19.71	17.12	14.13	13.15	12.83
		C_L	48.96	33.58	25.00	16.11	11.46	8.79	6.38	4.35	1.75	0.84	0.55

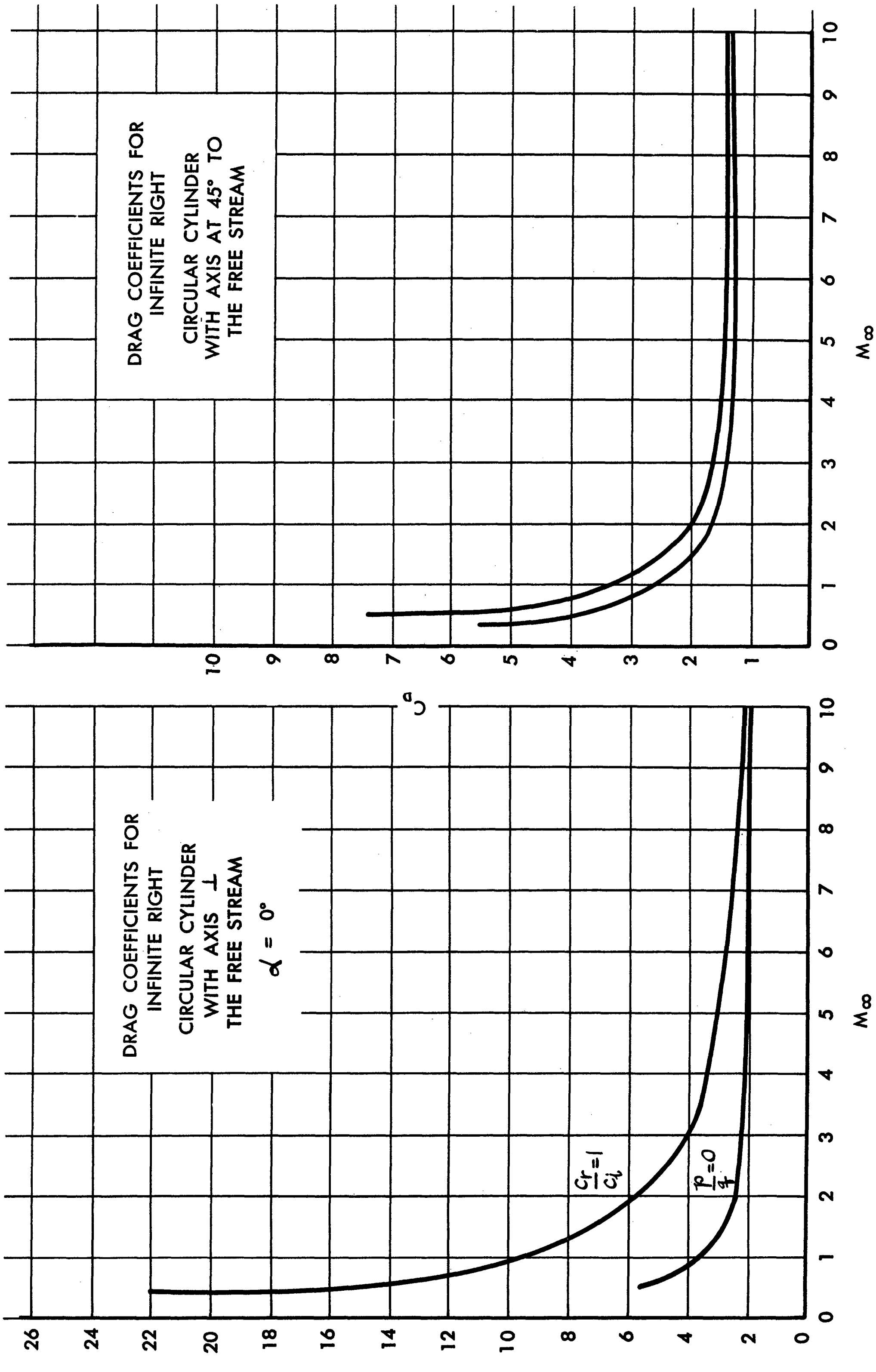
DRAG COEFFICIENTS FOR INFINITE RIGHT CIRCULAR CYLINDER WITH AXIS AT 45° TO THE FREE STREAM
DRAG COEFFICIENTS FOR INFINITE RIGHT CIRCULAR CYLINDER WITH AXIS ⊥ THE FREE STREAM
α = 0°
C_D
M_∞
$\frac{C_r}{C_i}=1$
$\frac{p}{q}=0$
0
1
2
3
4
5
6
7
8
9
10
12
14
16
18
20
22
24
26

FIG. 1

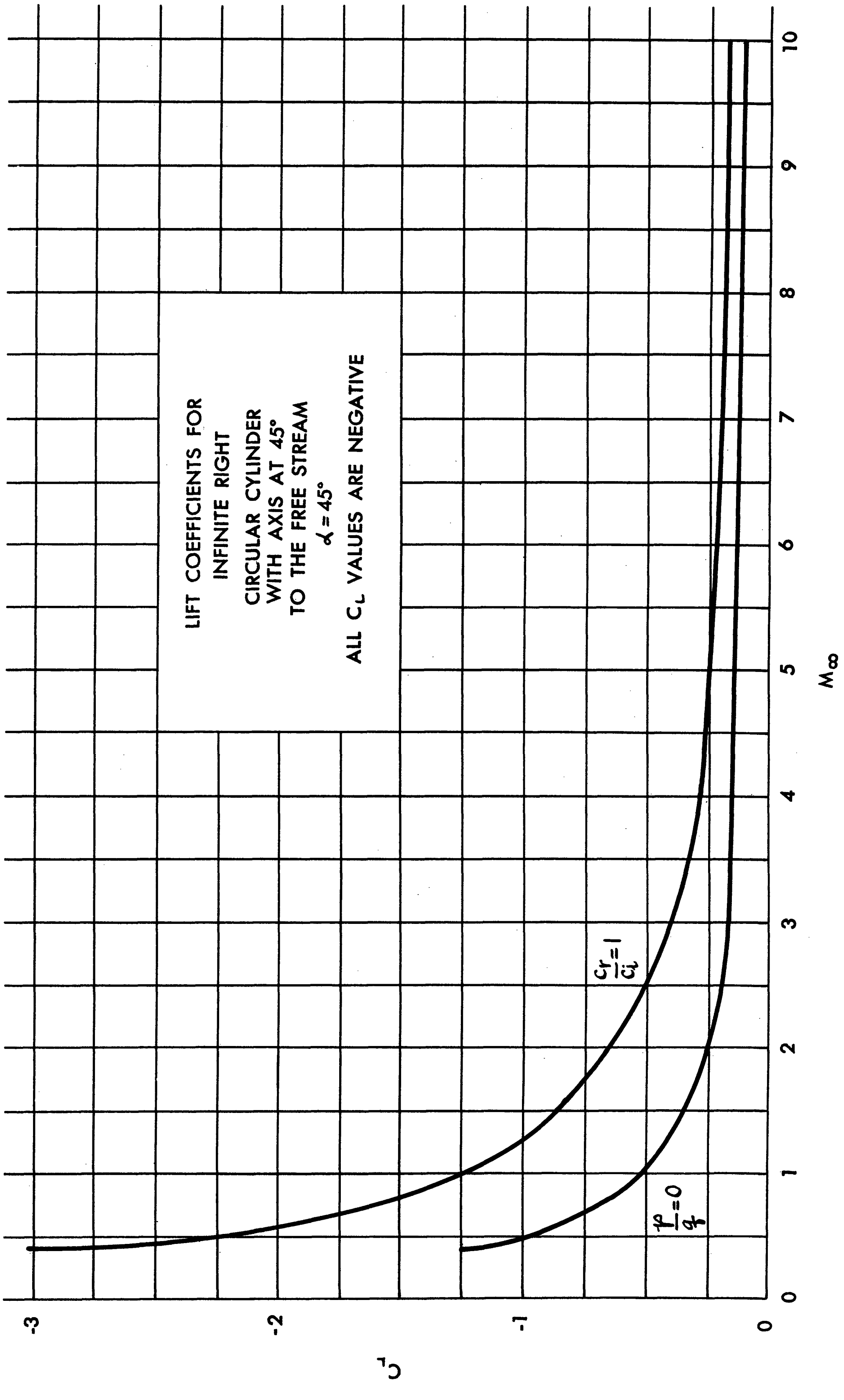
LIFT COEFFICIENTS FOR
INFINITE RIGHT
CIRCULAR CYLINDER
WITH AXIS AT 45°
TO THE FREE STREAM
$\alpha = 45°$
ALL C_L VALUES ARE NEGATIVE
$\frac{c_r}{c_i} = 1$
$\frac{p}{q} = 0$
M_∞
C_L
0
1
2
3
4
5
6
7
8
9
10
-3
-2
-1

FIG. 1 a

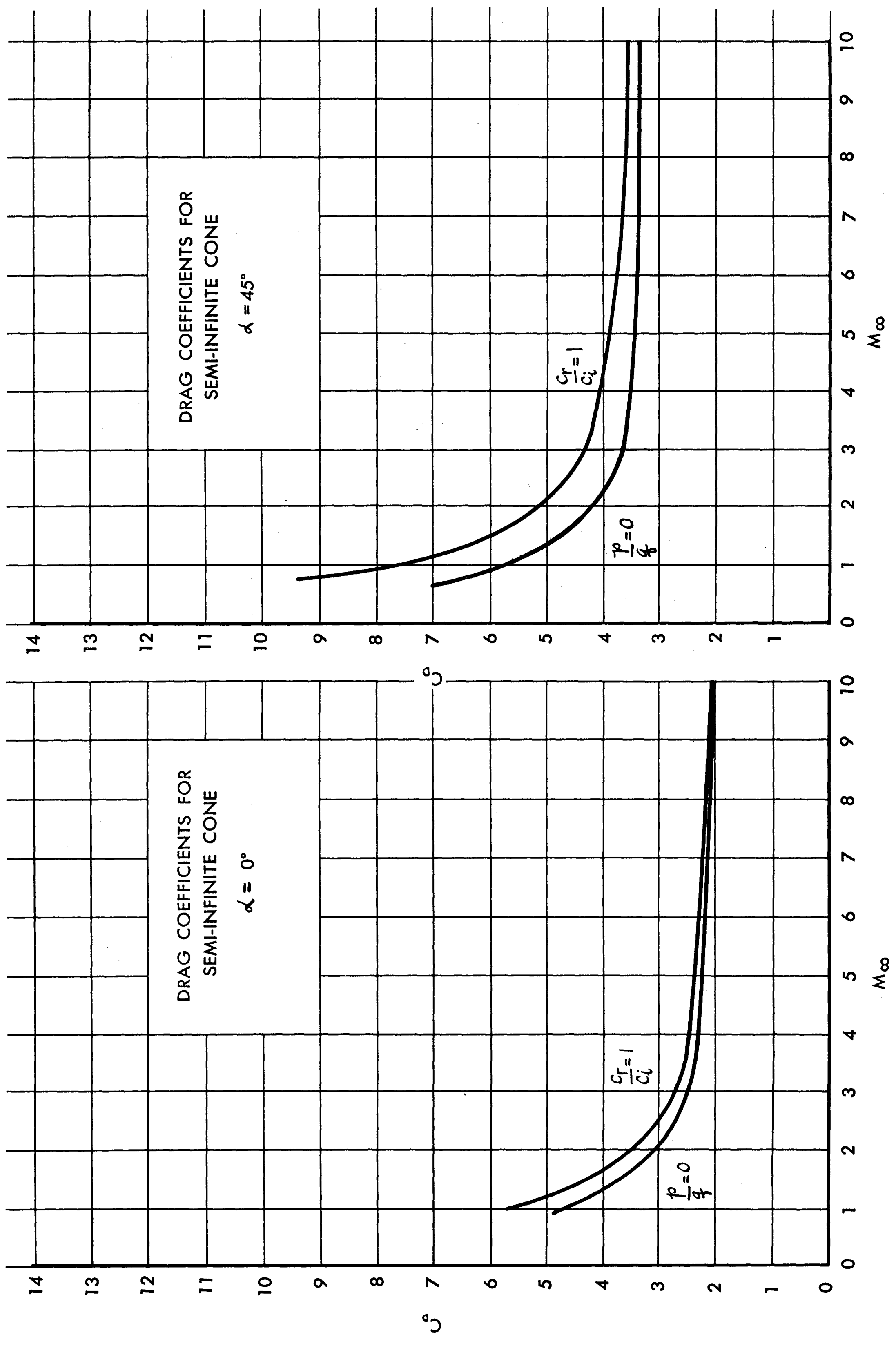
DRAG COEFFICIENTS FOR SEMI-INFINITE CONE
α = 45°
DRAG COEFFICIENTS FOR SEMI-INFINITE CONE
α = 0°
C_D
M_∞
$\frac{c_r}{c_i} = 1$
$\frac{p}{q} = 0$

FIG. 2

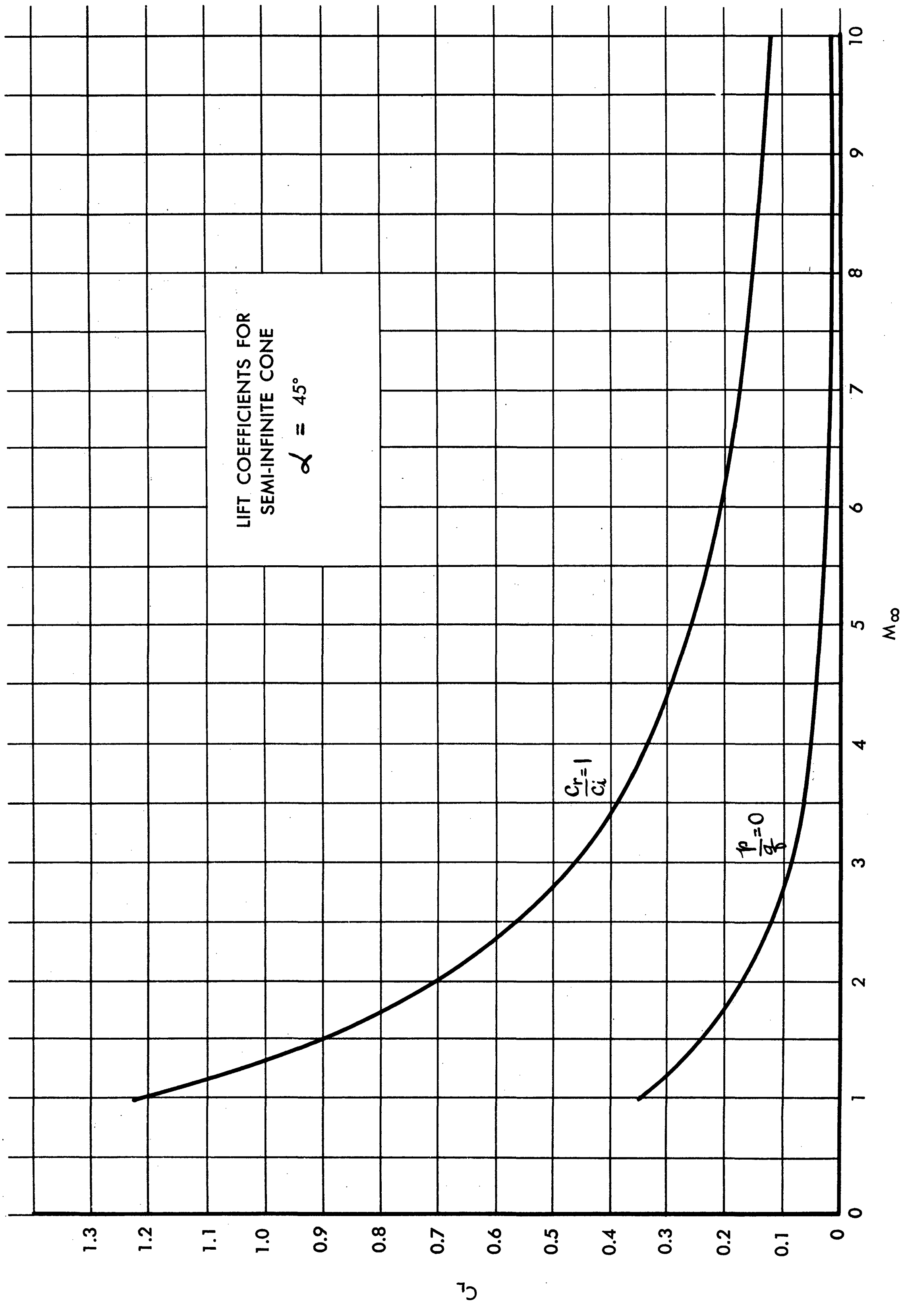
LIFT COEFFICIENTS FOR
SEMI-INFINITE CONE
α = 45°
$\frac{C_r}{C_i}=1$
$\frac{p}{q}=0$
C_L
M_∞
0
0.1
0.2
0.3
0.4
0.5
0.6
0.7
0.8
0.9
1.0
1.1
1.2
1.3
1
2
3
4
5
6
7
8
9
10

FIG. 2 a

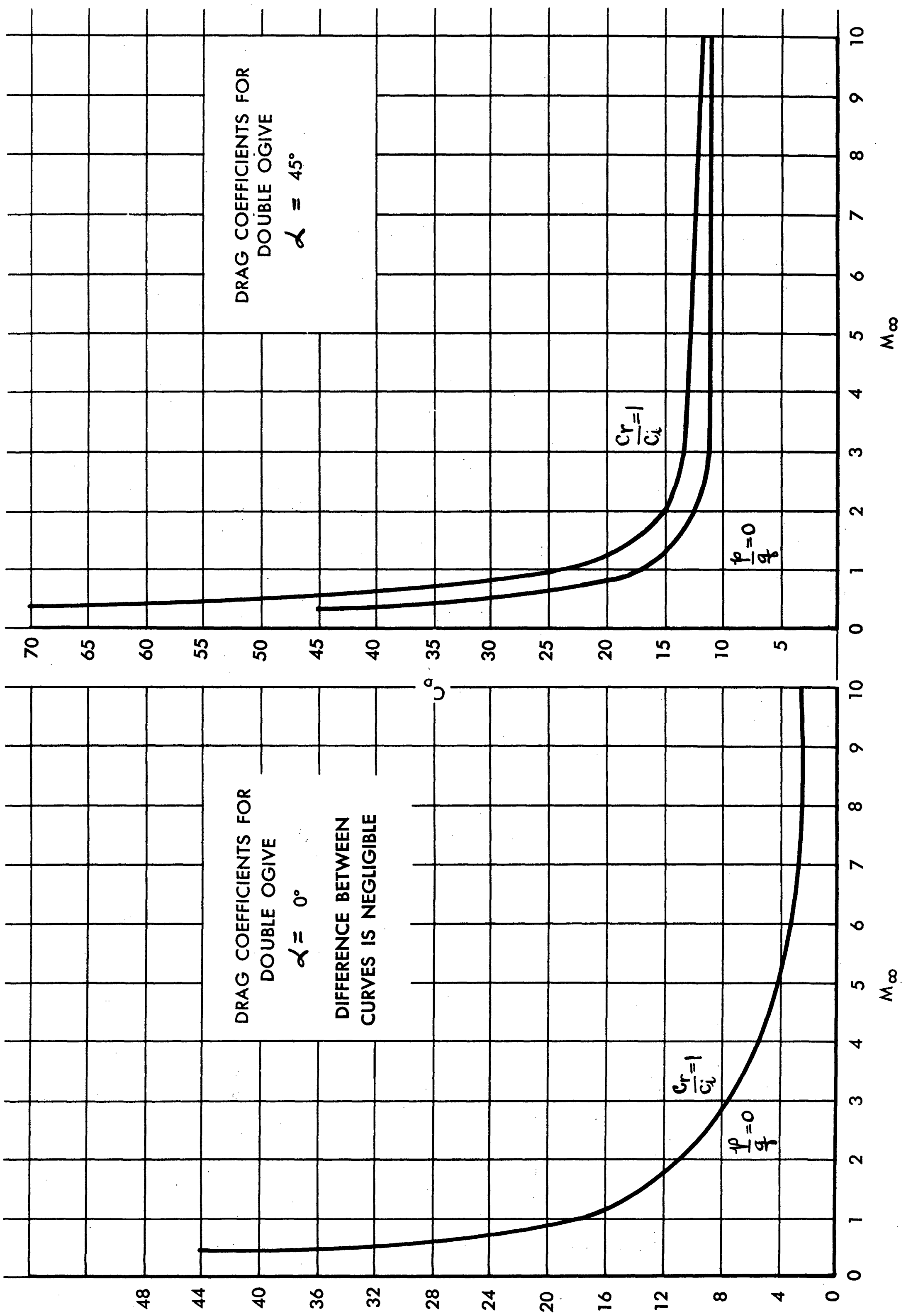
DRAG COEFFICIENTS FOR DOUBLE OGIVE
α = 45°
$\frac{C_r}{C_i} = 1$
$\frac{p}{q} = 0$
M_∞
C_D
DRAG COEFFICIENTS FOR DOUBLE OGIVE
α = 0°
DIFFERENCE BETWEEN CURVES IS NEGLIGIBLE
$\frac{C_r}{C_i} = 1$
$\frac{p}{q} = 0$
M_∞
C_D

FIG. 3

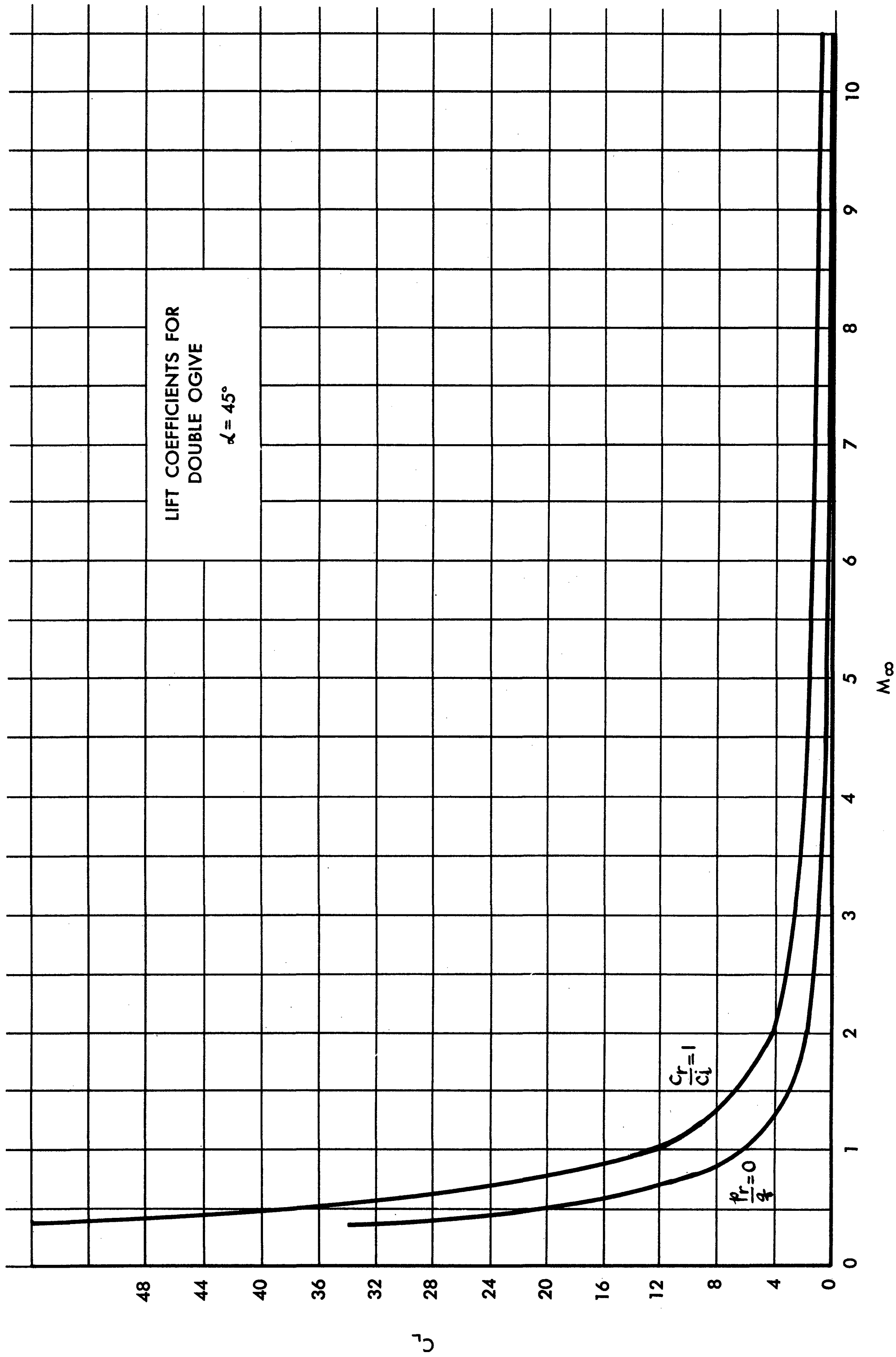
LIFT COEFFICIENTS FOR
DOUBLE OGIVE
α = 45°
$\frac{c_r}{c_t} = 1$
$\frac{p_r}{q} = 0$
M_∞
C_L
0
1
2
3
4
5
6
7
8
9
10
0
4
8
12
16
20
24
28
32
36
40
44
48

FIG. 3a

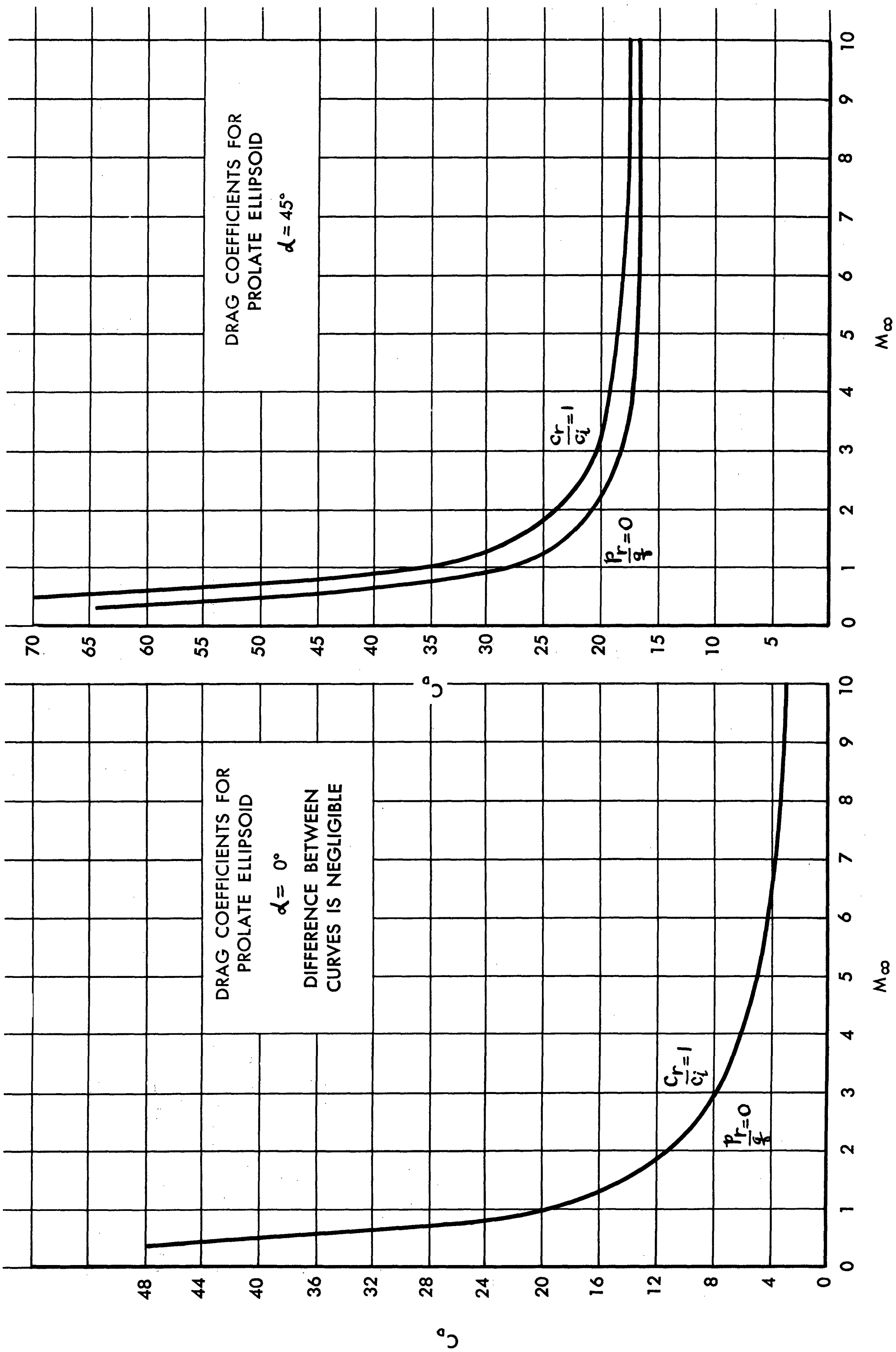
DRAG COEFFICIENTS FOR
PROLATE ELLIPSOID
α = 45°
$\frac{c_r}{c_i} = 1$
$\frac{p_r}{q} = 0$
DRAG COEFFICIENTS FOR
PROLATE ELLIPSOID
α = 0°
DIFFERENCE BETWEEN
CURVES IS NEGLIGIBLE
$\frac{c_r}{c_i} = 1$
$\frac{p_r}{q} = 0$
C_D
M_∞
0 1 2 3 4 5 6 7 8 9 10
70 65 60 55 50 45 40 35 30 25 20 15 10 5
48 44 40 36 32 28 24 20 16 12 8 4 0

FIG. 4

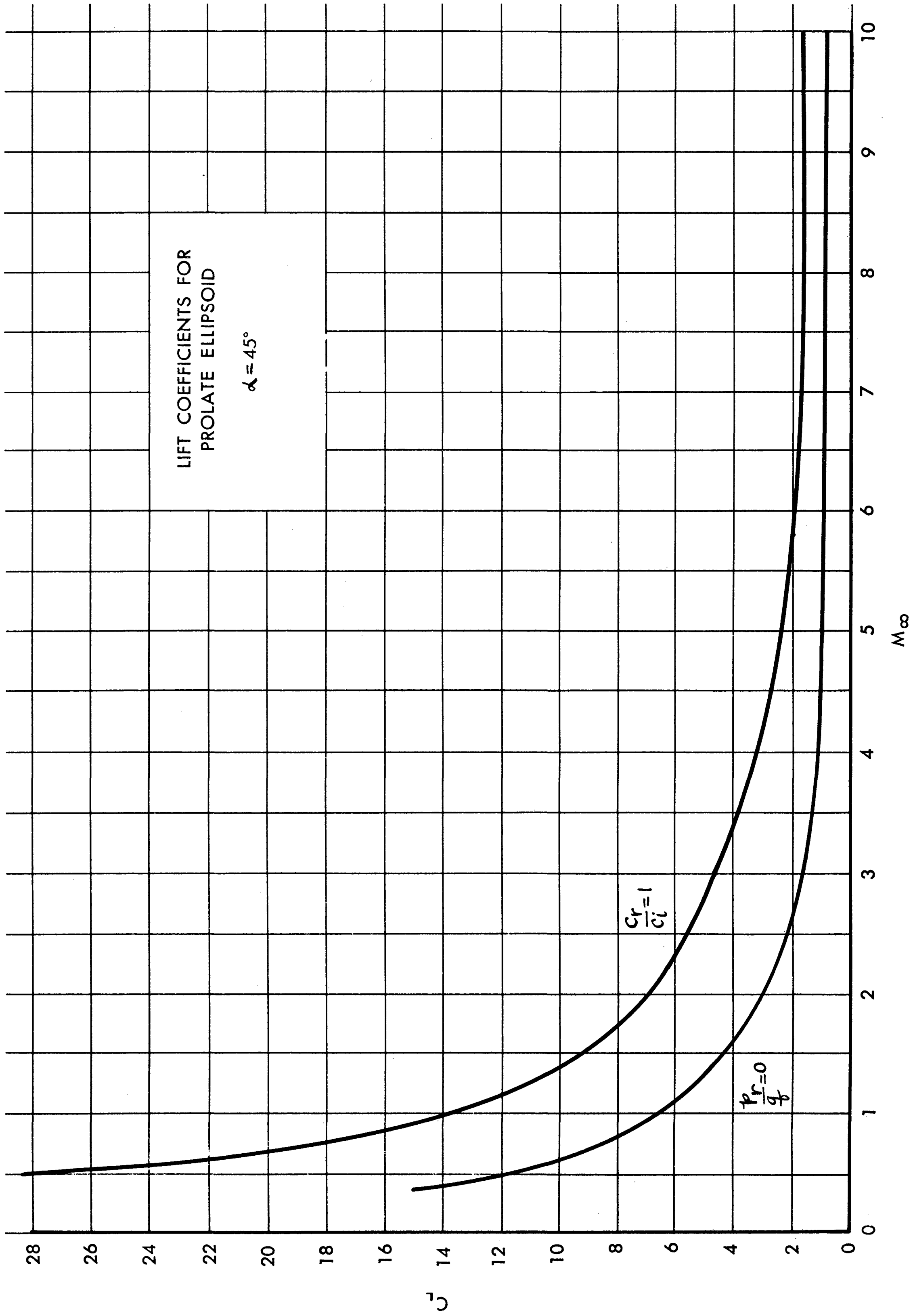
LIFT COEFFICIENTS FOR
PROLATE ELLIPSOID
$\alpha = 45°$
$\frac{c_r}{c_i} = 1$
$\frac{p_r}{q} = 0$
C_L
0 2 4 6 8 10 12 14 16 18 20 22 24 26 28
M_∞
0 1 2 3 4 5 6 7 8 9 10

FIG. 4 a

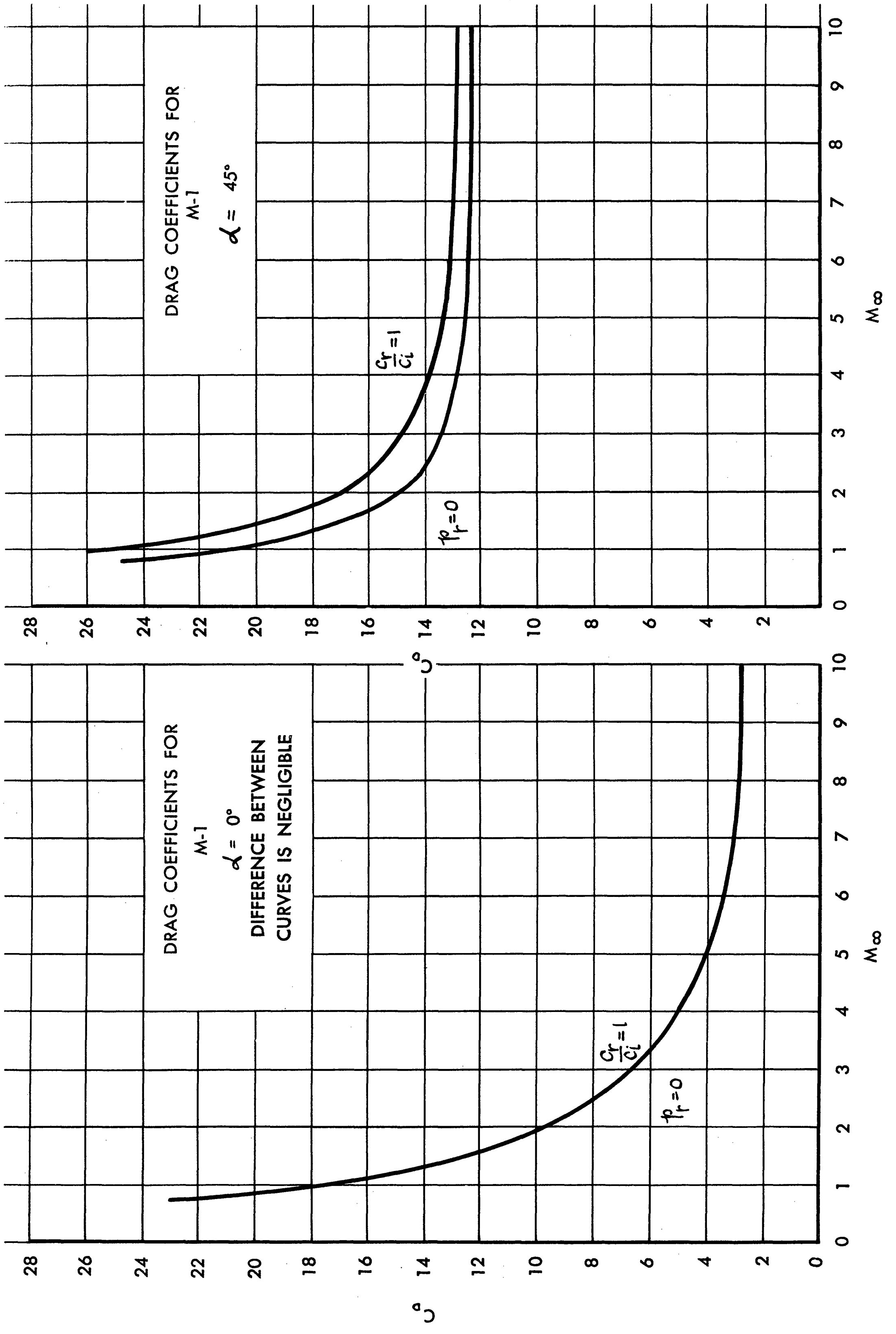
DRAG COEFFICIENTS FOR
M-1
α = 45°
$\frac{c_r}{c_i} = 1$
$p_r = 0$
DRAG COEFFICIENTS FOR
M-1
α = 0°
DIFFERENCE BETWEEN
CURVES IS NEGLIGIBLE
$\frac{c_r}{c_i} = 1$
$p_r = 0$
C_D
C_D
M_∞
M_∞
0
1
2
3
4
5
6
7
8
9
10
0
2
4
6
8
10
12
14
16
18
20
22
24
26
28

FIG. 5

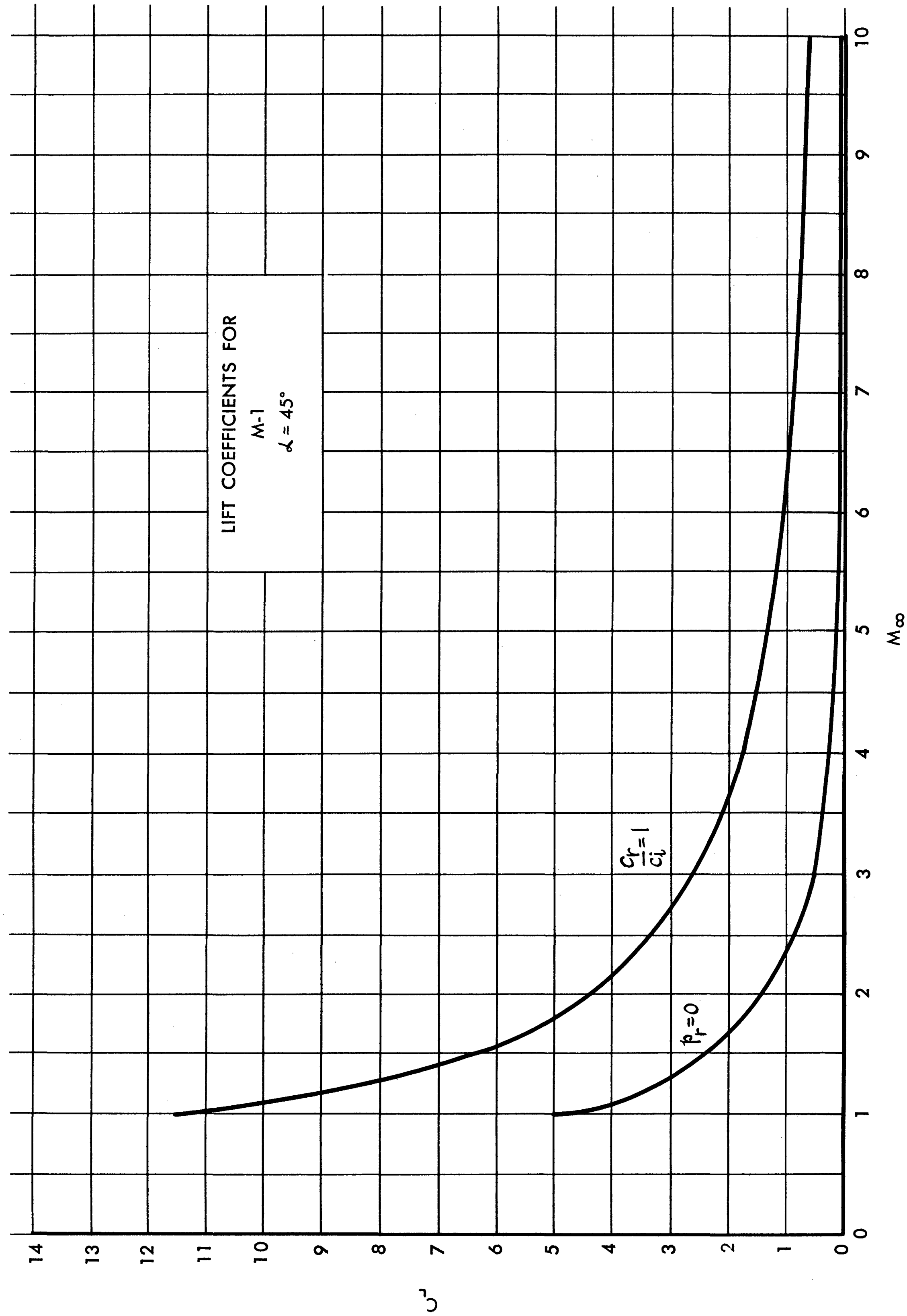
LIFT COEFFICIENTS FOR
M-1
α = 45°
$\frac{c_r}{c_i} = 1$
$p_r = 0$
M_∞
C_L
0
1
2
3
4
5
6
7
8
9
10
11
12
13
14

FIG. 5 a

DISTRIBUTION

Distribution of this report is made in accordance with ANAF-GM Mailing List No. 14, dated 15 January 1951, to include Part A, Part B and Part C.